https://doi.org/10.1016/j.engstruct.2021.112996

Experimental and numerical investigations on pre-twisted steel box-section columns

Feng Zhou [1,2], Yancheng Cai [3,*], Jun-feng Xu [2], Yiyi Chen [1,2], Yu Chen [1,2]

[1] *State Key Laboratory of Disaster Reduction in Civil Engineering, Tongji University, Shanghai 200092, China*

[2] *Department of Structural Engineering, Tongji University, 1239 Siping Road, Shanghai 200092, China*

[3] *Department of Civil and Environmental Engineering, The Hong Kong Polytechnic University, Hong Kong, China*

(Formerly, Department of Civil Engineering, University of Hong Kong, Pokfulam Rd., Hong Kong, China)

Abstract:

Experimental and numerical investigations on pre-twisted steel box-section columns are presented in this paper. A series of tests was conducted to investigate the effects of pre-twisted angle ratio on the compressive behaviour of steel box-section columns. The pre-twisted angle ratios of 3 °/m and 15 °/m were considered in the design of column specimens. The column specimens had effective lengths of 1.5 m and 4.0 m, and cross-section dimensions of 280 × 100 (depth × width) mm and 350 × 120 mm. A non-linear finite element model (FEM) considering geometric imperfections was developed. The results from the finite element analysis were compared with those from the column tests in terms of ultimate loads, failure modes and load-deformation curves. After successful verification, the FEM was employed to conduct an extensive parametric study on the structural behaviour of pre-twisted steel box-section columns. The key parameters in the parametric study included the pre-twisted angle ratios, ratios of depth to width in cross section, effective column lengths and end boundary conditions. It was shown that the pre-twisted angle ratios had little effect on the axial capacity, initial stiffness and lateral deformation capacity of shorter columns that failed by plastic yielding; however, more significant effects were found for the longer columns that failed by elastic flexural buckling. Theoretical analysis on the elastic buckling of pre-twisted steel box-section columns was conducted. Based on which, the formula for the buckling coefficient (reduction factor) was proposed that was suitable for the prediction of ultimate strength of pre-twisted steel box-section column.

Keywords: Experimental investigation; finite element analysis; pre-twisted column; steel box-section, ultimate load.

* E-mail address: yancheng.cai@polyu.edu.hk (Y. Cai)

1. Introduction

Pre-twisted structural members are widely used in engineering industry [1], such as propeller, helicopter and wind turbine. These rotating structures are twisted along the longitudinal direction in order to optimize the aerodynamic performance [2]. Research works on the nature of pre-twisting and its applications have been studied, including the theories on the behaviour of pre-twisted beams such as anisotropic beam theory [3], the extension of using Hamilton's principle and Galerkin's method in dynamic problem [4], the extension of the classical Saint-Venant approach [5]. These theories have been developed and utilized in different engineering fields, e.g., vibration in thermal environment.

Pre-twisting is a method of applying an angle of twist in the longitudinal direction of the member, where the principal axes of inertia rotates in accordance with the centroidal axis of the member. Moreover, the effects of pre-twisting can be explained as a transition between the weak and strong axes of the member, from which the original weak axis of the member may be strengthened while the original strong axis of the member may then become weaker after pre-twisting [5]. Figure 1 illustrates a structural member that has a natural twist in accordance with the centroidal axis along its longitudinal direction.

In the construction industry, pre-twisted structural members have been increasingly used due to the development of design, the pursuit of elegance, as well as the innovative concepts from both engineers and architects. Pre-twisted structural steel members have been used in engineering structures, such as the Beijing National Stadium known as the "Bird's Nest", and the World Expo Museum in Shanghai. The pre-twisting of the sections along the direction of the member length may vary in an arbitrary manner [7], e.g., pre-twisted with a constant or varied angle ratios. Nonetheless, structural performance of pre-twisted members has gained significant attention.

Investigations on the structural behaviour of pre-twisted column members have been carried out, but relatively limited. Fischer [8] investigated the influences of different moments of inertia and boundary conditions on the buckling loads of pre-twisted columns. Frisch-Fay [9] studied the stability of twisted bar under axial compression load. It was found that the critical load of the twisted bar was higher than that of the untwisted one. Similarly, the study on pre-twisted columns conducted by Tabarrok *et al.* [10] showed that the effects of the natural twist increased the first buckling load and diminished the second one. These observations were further proofed by the theoretical analysis carried out by Serra [11] that the pre-twisting can be taken into consideration as a simple way of strengthening compressed thin columns.

Effects of pre-twisting on statically determinate and indeterminate slender columns were investigated by Steinman *et al*. [12], where the general stability equations applied for a spatial rod were used as a part of the derived differential equations. The instability of pre-twisted columns subjected to static and periodic axial loads were investigated by Celep [13], where the static buckling loads and coefficients of the instability regions were presented. More recently, Barakat and Abed [14] conducted an extensive experimental investigation on the inelastic axial capacities of the pre-twisted steel bars, including over 200 specimens with rectangular cross sections. The data pool was then expanded by using non-linear finite element analysis to include a wider range of pre-twisting angles up to 270° [15]. Mathematic models were developed by multiple regression analysis that could predict well the critical loads of the pre-twisted bars. The research work was further extended to the elastic buckling capacities of pre-twisted columns with universal sections, i.e., I sections, by finite element analysis [16].

However, it should be noted that up to date, there has few investigations on the structural behaviour of pre-twisted steel box-section columns, which are one of the commonly used members in steel structures. Furthermore, the current international specifications, such as Eurocode (Eurocode 3: Design of steel structures) [17], American Specification (Specification for Structural Steel Buildings. ANSI/AISC 360-16) [18] and Chinese Code (Code for design of steel structures. GB 50017-2017) [19], do not provide design rules for pre-twisted members, e.g., tubular columns. In this study, experimental and numerical investigations on pre-twisted steel box-section columns were carried out.

Firstly, a series of short and long pre-twisted steel columns with box-sections was tested. The box-sections were fabricated by welding the heat-treated structural steel plates. The grades of steel plates were Q235 and Q345 with the nominal yield stresses of 235 MPa and 345 MPa, respectively. Secondly, a verified non-linear finite element model (FEM) was developed to conduct an extensive parametric study on the structural behaviour of pre-twisted steel box-section columns. The key parameters in the parametric study included the pre-twisted angle ratios, ratios of section depth to width, effective column lengths and end boundary conditions. The effects of the key parameters on the structural behaviour of the pre-twisted steel box-section columns were investigated. Lastly, theoretical analysis on the pre-twisted steel box-section columns was conducted. A formula for the stability coefficient (reduction factor) was proposed for the ultimate loads of pre-twisted steel box-section columns with pin-end boundary conditions. The purpose of this study is to provide valuable findings on the structural behaviour of pre-twisted steel box-section columns and facilitate their applications in practice.

2. Experimental investigation

2.1 Test specimens

A series of tests was conducted on pre-twisted steel box-section columns. The box-sections were fabricated by welding the heat-treated structural steel plates. The grades of steel plates were Q235 and Q345 with the nominal yield stresses of 235 MPa and 345 MPa, respectively. The thicknesses of the steel plates are 10 mm and 16 mm for Q235, and 12 mm and 20 mm for Q345. The plate thicknesses of 10 mm and 16 mm with grade Q235 were used to fabricate Section (h×b×t_w×t_f) 280×100×10×16, while the plate thicknesses of 12 mm and 20 mm with grade Q345 were used to fabricate Section (h×b×t_w×t_f) 350×120×12×20. In which h is the overall web depth, b is the overall flange width, t_w and t_f are the thickness of the web plate and flange plate, respectively. The symbols of a cross section (h×b×t_w×t_f) without pre-twisting are defined in Figure 2. The steel plates were pre-deformed by given cross section angle ratios of 3 °/m or 15 °/m along the member length. After pre-deformed, the steel plates were positioned to form the box-section by welding. The box-section dimensions (depth × width) of columns are 280×100 mm and 350×120 mm. Six pre-twisted steel box-section columns were designed covering different steel grades, column effective lengths (L_e), pre-twisted angle ratios (ϕ), section dimensions and slenderness (λ). The angle ratio of 15 °/m was the maximum ratio that could be manufactured (pre-twisted) in the factory while the smaller angle ratio of 3 °/m was designed as a comparison. Two nominal lengths (L) of 1220 and 3410 mm were considered for the pre-twisted short and long steel box-section columns, respectively.

The details of the test specimens are shown in Table 1. The columns were labelled by three segments. For example of Specimen 280×100×10×16-1.5-ϕ3, the first segment means the column section dimensions of 280×100×10×16 mm; the second segment stands for the effective length (L_e) of 1.5 m for the column specimen; and the last segment means the pre-twisted angle ratio of 3 °/m considered for the column specimen. If it is a steel column without pre-twisting, then it is indicated by the term of $\phi 0$.

2.2 Fabrication of pre-twisted steel box-section column specimens

There are commonly two ways to fabricate a pre-twisted steel box-section column, i.e., twist a steel box-section column, or deform the steel plates and then assemble the pre-deformed steel plates to form a pre-twisted box-section column. To minimise the residual stresses and the welding deformation developed during the forming process, the second method was used in this study to fabricate the pre-twisted steel box-section columns.

Firstly, the steel plates were pre-deformed by following the pre-twisted steel box-section column dimensions and further heat treated (temperature within 500 ~ 900 ^{o}C) in the factory. According to the dimensions of the pre-twisted steel box-section columns, the steel moulds were designed and fabricated for assembling the pre-deformed steel plates to form the pre-twisted box-section columns. The coordinates of the moulds were carefully checked such that the errors were within the limit of $\pm$0.2 mm. Then, one pre-deformed web plate of the steel box-section column was put into the moulds. The positions of the web were double checked with the designed coordinates in the moulds, where the errors were controlled within $\pm$1.0 mm. Pyrotechnics heating was adopted to correct the positions of the pre-deformed steel web such that they were positioned in the accurate coordinates. After that, two pre-deformed flanges of the box-section columns were then put into positions. The two flanges with the positioned web formed the U-shape of the pre-twisted sections. In this stage, temporary steel plates were set in positions inside the pre-twisted steel sections. The pre-deformed web was welded with the two pre-deformed flanges. The accurate positions of the U-shape were checked against with the control points. Finally, the last pre-deformed web of the box-section was positioned. Spot welding was used at certain locations along the column length. The positions of the moulds and heat input during welding were carefully adjusted such that the deformation due to welding process was minimized. The accurate positions of the fabricated pre-twisted steel box-section columns were double checked after welding completed. Similar to the corrections of the pre-deformed steel plates, pyrotechnics heating was also used for the adjustments of the fabricated column specimens by referring to the coordinates in the moulds. It should be noted that all the pre-twisted steel box-section column specimens were designed and fabricated such that the cross sections at the mid-height were not twisted. In other words, twisting of the column sections may be viewed from the position (un-twisted cross-section) that is at the middle length towards the two ends.

2.3 Material properties

The material properties of the steel column specimens were determined by tensile coupon tests. The plate thicknesses of 10 mm and 16 mm were used to fabricate Section 280×100×10×16, while the plate thicknesses of 12 mm and 20 mm were used to fabricate Section 350×120×12×20. Tensile coupon specimens were extracted from the original (without twisting) steel plates. The specimens were cut in the direction that was perpendicular to the rolling direction of the steel plates, in accordance with the GB/T 2975-1998 [20]. For each thickness of the steel plate, three tensile coupon specimens were tested to determine its material properties. Hence, a total of twelve tensile coupons were tested for the four different thicknesses of steel plates. The tensile coupon specimens were prepared and tested according to the GB/T 228-2002 [21].

A calibrated extensometer of 50 mm gauge length was used to measure the longitudinal strain of the coupon specimens. A data acquisition system was used to record the load and the strain readings at regular intervals during the tests. The material properties based on the averages of the three coupon test results for each plate thickness were summarized in Table 2. These includes the initial Young's modulus (E), the yield stress (f_y), the tensile strength (f_u), ultimate strain (ε_u) and the elongation after fracture (ε_f) based on a gauge length of 50 mm.

2.4 Test rig and results

Experimental investigation on the pre-twisted steel box-section columns was conducted by applying axial loads at the column ends. The short columns (L_e = 1.5 m) were tested in a universal testing machine with a capacity of 30000 kN. The long columns (L_e = 4.0 m) were tested by using a 2000 kN servo-controlled hydraulic actuator. The schematic views of the test setup for short and long columns are illustrated in Figures 3a and 3b, respectively. The steel end plates with thickness of 30 mm were welded to both ends of the specimens to prevent the local failure at the specimen ends, and also transfer loads to the cross sections. The steel end plates were then fixed to the loading plates by bolted connections. For short columns, the specimen tests were designed with half-rounded supports at both ends, where the short columns were free in rotation about the minor axis of un-twisted cross section (cross section at mid-height). The column ends were fixed in other degrees of freedom except that the top was free in vertical direction. The axial load was applied into the column by moving the cross head of the testing machine. Similar end boundary conditions were applied to the long columns, where the degree of freedom in rotation about the minor axis of un-twisted cross section was provided by the pin-end shrank at both ends of the column. The effective lengths (L_e) of the short and long columns were determined by considering the depths of the half-rounded supports and the distance between the centres of the pins, respectively. Hence, the respective L_e of short and long box-section columns were set as 1.5 m and 4.0 m in this study. Two 50 mm range Linear Variable Displacement Transducers (LVDTs) were used to measure the column deflections in the middle length. At each column end, another two 50 mm LVDTs were set to measure the rotation of the column about its minor axis. The axial shortening of the columns were obtained by the four LVDTs at the two ends.

A preload of around 10% of the estimated box-section column capacity was applied to check the test instrumentations and setup. The box-section column was then un-loaded. In the real test, the box-section column was loaded by displacement control with a loading rate of 1.0 mm/min until the ultimate load (P_t) was reached. After that, the test was stopped when the load applied on the box-section column dropped over 15% of the ultimate load (P_t). A data acquisition system was used to record the applied loads, axial deformations and lateral deflections at regular intervals during the tests. The ultimate loads (P_t) with the corresponding end shortenings (δ_t) and the failure modes of the pre-twisted steel box-section columns were summarized in Table 3, where the calculated yield strengths (P_y) of the cross sections without pre-twisting were also included. The yield strength (P_y) is the sum of the web areas and flange areas times their respective yield stress in the cross section. Figures 4a and 5a illustrate the failure modes of short column Specimen 350×120×12×20-1.5-ϕ3 and long column Specimen 280×100×10×16-4.0-ϕ15, respectively. Figure 6 shows the load versus end shortening curves for all the tested column specimens. All tested columns showed clear peak loads from the load-deformation curves. The short columns were failed in plastic yielding of the cross section. For short column, the stresses on the cross section generally reached the yield stress (f_y) at the ultimate point of the column curve (peak load) and small flexural deformation was also observed at the post-ultimate stage. It should be noted that the yield stress corresponds to the onset of plasticity, while ultimate stress corresponds to the maximum tensile capacity according to the steel stress-strain curve obtained from the tensile coupon test. However, the long columns were failed in elastic flexural buckling, and quite large flexural deformation was observed even before the ultimate. For both short and long pre-twisted columns, the flexural deformation mainly occurred in the plane about the weak axis of un-twisted cross section (cross section at mid-height). It should also be noted that no local buckling was found in the long columns. For short columns, the pre-twisted steel box-section columns with larger ratio of pre-twisted angle had similar ultimate loads compared with those with smaller ratio of pre-twisted angle, e.g., the P_t = 2105 kN for Specimen 280×100×10×16-1.5-ϕ15 compared with P_t = 1971 kN for Specimen 280×100×10×16-1.5-ϕ3. However, the pre-twisted angle ratio could obviously improve the axial capacities of long pre-twisted steel box-section columns, i.e., the 2000 kN for Specimen 280×100×10×16-4.0-ϕ15 compared with 1436 kN for Specimen

280×100×10×16-4.0-ϕ3. This could be due to that the failure of the long columns were dominated by flexure buckling about the minor axis. For the column with larger pre-twisted angle ratio, (i.e., ϕ = 15 °/m compared with ϕ = 3 °/m), the section flexural rigidity of the column along the longitudinal direction (started from the middle length) was more improved, by comparing with that of column without pre-twisting for Section 280×100×10×16 in this study. Hence, the ultimate load corresponding to the flexural buckling failure was improved. In addition, the pre-twisted column would produce the torsional deformation together with its axial deformation and flexural deformation. The torsional deformation affected the free rotation of the pin-ends during testing, which made the columns ends towards fix-end boundary conditions, resulting in higher flexural buckling load. These will be discussed further in detail in the later sections of this paper.

3. Finite element model

3.1 Development of finite element model

The non-linear finite element program ABAQUS Version 6.12 [22] was used to simulate the structural behaviour of the pre-twisted steel box-section column specimens. The finite element model (FEM) was developed and analysed in two steps. In the first step, linear perturbation analysis was performed on FEM with a "perfect" geometry to obtain probable elastic buckling modes of the pre-twisted steel box-section columns. The elastic section and member buckling mode patterns were obtained by performing eigenvalue analysis in BUCKLE procedure. The buckling mode pattern was amplified by a certain magnitude of imperfection to consider the initial geometric imperfection profile of the steel box-section columns. In the second step, finite element analysis was performed by considering the non-linearities of both the geometry and material properties. The ultimate loads, lateral and axial deformations, and the failure modes of pre-twisted steel box-section columns were obtained.

In the FEM, the measured specimen dimensions and the material properties obtained from the tensile coupon tests were used. The model was developed based on the centreline dimensions of the cross sections. The pre-twisting was achieved by checking the "twist, pitch" option and entering the corresponding pre-twisted ratio when editing the base extrusion. In the ABAQUS [22], the "twist" modifies an extrusion by rotating the sketched profile about an axis parallel to the direction of extrusion, while the "pitch" defines the extrusion distance in which the profile would be twisted. The measured engineering stress-strain curves were converted into real stress-strain curves. The von Mises yield criterion along with the associated flow rule was used for the multiaxial stress state [23]. Residual stress for welded steel box sections was considered in the FEM for the sensitivity study. The models of parabolic profile and polygon profile for the residual stress in the cross section of steel boxing columns have been investigated in the reference [24]. Generally, it was found that the residual stress had little effect on the ultimate capacity of the steel boxing columns under axial loading. In this study, the model of polygon profile in the reference [24] for welded box sections was adopted in the verification of the FEM using the ABAQUS (*INITIAL CONDITIONS, TYPE=STRESS) parameter to assess the influence of the residual stresses. Similarly, it was found that the residual stress had little effect on the ultimate loads of the pre-twisted steel box-section columns.

The pre-twisted steel box-section column was modelled using the four-node shell (S4R) element with reduced integration. The finite element mesh size of 10×10 mm (length × width) was used for all specimens. Such mesh size was selected based on a series of sensitivity studies by varying the size of the elements to provide both accurate results and less computational time. In addition, a scale factor of $t/500$ and $3L_e/1000$ was chosen for local (section) geometric imperfection amplitude and for overall (member) geometric imperfection amplitude, respectively, in modelling the pre-twisted steel box-section columns. The fundamental local and overall buckling modes obtained in the first step of the analysis were used. Hence, both local and overall geometric imperfections have been incorporated in the FEM.

The axial compressive force was applied through the end plates of the specimen. The end plates were modelled using analytical rigid plates because no deformation failure was found in the end plates in the tests. The “tie constraint pair” was modelled in the interfaces between the end plates and the ends of column cross section. The end plates were defined as the master surface while the column cross sections were defined as the slave surface in the FEM. The “tie constraint” ties two surfaces together, which enable the pair of surfaces shares the same translational and rotational degrees of freedom.

Following the boundary conditions of the column tests, the top end plate was restrained against all degrees of freedom, except for the degree of freedom in rotation about the minor axis of the un-twisted cross section as well as the degree of freedom in translation in the vertical direction. The bottom end plate was restrained against all degrees of freedom except for the degree of freedom in rotation about the minor axis of the un-twisted cross section. The boundary conditions were assigned to the reference points of the end plates. Similar to the displacement control method used in the pre-twisted column tests, the load was applied to the specimens by specifying a displacement to the reference point of the analytical rigid plate in the FEM.

3.2 Verification of FEM

The ultimate loads (P_{FEA}) predicted from the finite element analysis (FEA) and those obtained from the tests (P_t) were compared, as shown in Table 4(a). For the short columns, the mean value of P_t/P_{FEA} is 0.97 with the coefficient of variation (COV) of 0.028. For the long columns, the results from the FEA are lower than those from the tests. The main reason is that the torsional deformation at the ends of the long pre-twisted columns was intended to occur during the tests, which would constrain the rotation of the column ends to some extent (see Figure 4b). Hence, the pin-end boundary conditions of the column ends about the weak axis converted to semi-rigid resulting in larger flexural buckling load, where such end boundary condition effects were not modelled in the analysis. However, the effects of the boundary conditions will be further analysed in the later paragraph. Nonetheless, it was shown that the results from the FEA could generally predict the structural behaviour of the pre-twisted steel box-section columns in terms of the load-end shortening curves and the failure modes. The load versus end shortening curves between test and FE results were shown in Figure 7(a), where the initial part of the test curve was well predicted by the FE result. Figure 4 and Figure 5 showed the comparison of failure modes between the tested columns and FEA columns.

In order to investigate the effects of boundary condition on the load-end shortening response and ultimate load of the pre-twisted members, the rotation stiffness about the minor axis of the twisted cross section subjected to axial loading was further analysed. In the analysis, only the rotation stiffness about the minor axis was considered. The seven cases of rotation stiffness are 0 (pin end), 0.1×10^6, 0.5×10^6, 1×10^6, 5×10^6, 10×10^6 (N.m/rad) and ∞ (fix end). Two standard springs were assigned to the reference point at each column end for the degree of freedom in rotation about the minor axis of the cross section. The FE models of the long pre-twisted steel specimens 280×100×10×16-4.0-ϕ3 and 280×100×10×16-4.0-ϕ15 were used in the investigation. The obtained ultimate loads were tabulated in Table 4(b). The load-end shortening curves were plot in Figures 7(b)-(c), for specimens 280×100×10×16-4.0-ϕ3 and 280×100×10×16-4.0-ϕ15, respectively. It is shown that as the rotation stiffness increased, the ultimate load of the specimen increased. The ultimate loads of columns with rotation stiffness of ∞ (fix end) are 95% and 81% higher than those with rotation stiffness of 0 (pin end), for specimens 280×100×10×16-4.0-ϕ3 and 280×100×10×16-4.0-ϕ15, respectively. The stiffer boundary conditions provided more constrains to the torsional deformation at the ends of the long pre-twisted columns, hence the column ultimate capacity increased. This explains why the FE results for specimens 280×100×10×16-4.0-ϕ3 and 280×100×10×16-4.0-ϕ15 in Table 4(a) underestimate the test ultimate loads of these two columns due to the end boundary conditions as discussed previously. It should be noted that this study mainly focused on the pre-twisted steel box-section columns subjected to axial loading, where the columns are free to rotate about the minor axis of the un-twisted cross section which located at the middle height of the column. Hence, in the parametric analysis of the paper, the pin end boundary conditions (i.e., rotation stiffness of 0) about the minor axis of the un-twisted cross section were assigned to the column ends.

4. Parametric analysis and discussions

4.1 General

The verified FEM was employed to conduct the parametric study on the structural behaviour of the pre-twisted steel box-section columns. The key parameters considered in the specimen designs included the pre-twisted angle ratios (ϕ), ratios of overall web depth to overall flange width (h/b) in the cross section, effective column lengths (L_e) and end boundary conditions. The details of the pre-twisted steel box-section columns are illustrated in Tables 5a-5c. For the key parameter of ϕ with different L_e, the specimens of the same Section 280×100×10×16 ($h \times b \times t_w \times t_f$) mm were designed (See Table 5a). The specimens were divided into five groups by the values of L_e; For the effects of ϕ with different h/b, five different sections with the constant values of t_w = 10 mm and t_f = 16 mm were designed (See Table 5b), where two different effective column lengths (L_e= 1.0 m and L_e= 4.0 m) were considered; For the effects of ϕ with different end boundary conditions, the specimens of the Section 280×100×10×16 mm with L_e= 4.0 m were used (See Table 5c). Overall, the pre-twisted angle ratios were designed to cover a wide range in each column series, e.g., from 0 to 100 °/m. Generally, pin-end boundary conditions with free rotation about the minor axis of the un-twisted sections were assigned to all the specimens, except for those specimens in Table 5c. These specimens were assigned pin-end boundary conditions with free rotation about both minor and major axes of the un-twisted sections. Similar to the test specimens, all the pre-twisted steel box-section column specimens in the parametric study were designed such that the cross sections at the mid-height of the specimens were un-twisted. The converted real stress-strain curves of steel plates with thicknesses of 10 mm and 16 mm were used for the respective webs and flanges in the parametric study.

4.2 Effects of ϕ with different L_e

The ultimate loads and failure modes of specimens in Table 5a were detailed in Tables 6a-6e. The ultimate loads of columns with pre-twisted angle ratios were normalized with those of columns without pre-twisting ($\phi = 0$) in each series. Figures 8a and 8b illustrated the load-deformation curves for pre-twisted steel box-section column (Section 280×100×10×16 mm) with effective length (L_e) of 1.0 m and 4.0 m, respectively. In each figure, the curves for columns with different values of ϕ were included. It was shown that the values of ϕ had little effect on the initial stiffness of the columns regardless of different effective lengths. The values of ϕ had little effect on the ultimate loads of the relatively short columns (L_e = 1.0 m); on the contrary, for the relatively long columns (L_e = 4.0 m), the effects of ϕ on the ultimate loads were obvious, i.e., the larger values of ϕ up to a certain limit, the larger ultimate loads of columns were obtained. The reason may be, as discussed in Section 2.4 of this paper, the failure of the long columns was dominated by the flexure buckling about the minor axis of the un-twisted section. For the columns with larger values of ϕ, the section flexural rigidities of the columns along the longitudinal direction (started from the mid-height) were more increased by comparing with those of columns without pre-twisting. Hence, the ultimate loads corresponding to the flexural buckling failure were improved. This will be discussed further in Section 4.6 of the paper.

Figure 9 shows the effects of ϕ on the ultimate loads of pre-twisted steel box-section columns for the specimens in Table 5a. The vertical axis plots the ultimate loads of columns normalized (P_{FEA}) with the ultimate loads of the column without pre-twisting ($P_{non\text{-}twisted}$). The horizontal axis shows the pre-twisted angle ratio (ϕ) of the columns. In the figure, the columns with the five different effective lengths (L_e) are included. For the relatively short columns (1.0 ~ 2.0 m), it was found that for the ϕ ranged from 0 to 30 °/m, the differences of ultimate loads were small, i.e., less than 1.0%. As the ϕ increased, the ultimate loads generally decreased, in particular for short columns with L_e = 1.0 m and L_e = 1.5 m. The ultimate loads decreased over 5% when the ϕ = 120 °/m. For the relatively long columns (3.0 ~ 4.0 m), it was shown that the ultimate loads increased with the larger values of ϕ (see Figure 9), namely, up to ϕ = 110 °/m for the specimen Series 280×100×10×16-3.0 and up to ϕ = 90 °/m for the specimen Series 280×100×10×16-4.0. This means that for a relatively long column, there is an optimum pre-twisted ratio for obtaining the maximum ultimate load.

Figure 10 further illustrates the relationship between the ultimate loads of the pre-twisted steel box-section columns and the column slenderness (λ) under different values of ϕ, for those specimens in Table 5a. The vertical axis plots the ultimate loads (P_{FEA}) of the columns normalized with the cross section strength (Af_y), i.e., P_{FEA}/Af_y, where A is the full area of the cross section. It was found that the relatively small values of ϕ (e.g., ϕ = 3 and 15 °/m) had little effect on the ultimate loads of the columns regardless of different column slenderness. Furthermore, it was shown that the ratios of P_{FEA}/Af_y intersected at λ = 50.59 for different values of ϕ, which meant that the columns with the same L_e had the similar ultimate loads in this study when λ = 50.59 regardless of different pre-twisted angle ratios (ϕ). Generally, for pre-twisted steel box-section columns with λ < 50.59, the values of P_{FEA}/Af_y decreased as the values of ϕ increased; however, when λ > 50.59, the values of P_{FEA}/Af_y increased as the values of ϕ increased. That means the pre-twisting along the steel columns improved the column stability under axial loading condition, which may be due to the improved section flexural rigidity along the column length as compared with columns without pre-twisting.

4.3 Effects of ϕ with different h/b ratios

Tables 7a-7e show the parametric study results of pre-twisted steel box-section columns (specimens in Table 5b), with the variations of ϕ, h/b and L_e. The effects of ϕ with different h/b on the ultimate loads of columns are summarized in Figures 11a and 11b, for L_e = 1.0 m and L_e = 4.0 m, respectively. The vertical axis of the figures plots the values of normalized ultimate loads, i.e., ultimate loads of columns (P_{FEA}) normalized with those of columns without pre-twisting ($P_{non\text{-}twisted}$) for the same series. The horizontal axis of the figures shows the pre-twisted angle ratios (ϕ). For the relatively short columns (L_e = 1.0 m) with $h/b \leq 2.8$ as shown in Figure 11a, it was found that the ratios of h/b had little effect on the ultimate loads when the ratios of $\phi \leq 50$ °/m. However, when the ratios of $\phi \geq 50$ °/m, the ultimate loads started to decrease, with the larger ratios of h/b (up to h/b = 2.8) the more decrement of the ultimate loads. For the relatively long columns (L_e = 4.0 m), generally, the larger ratios of h/b (up to h/b = 2.8), the more increment of the ultimate loads under the same ϕ was, e.g., for ϕ = 100 °/m, the increase of around 20% for section 150×100×10×16 (h/b = 1.5) compared with that of 22% for section 280×100×10×16 (h/b = 2.8), as shown in Figure 11b. For the ratio of h/b = 1.0, it was shown that the values of ϕ had little effect on the ultimate loads of the columns. This could be due to the relatively smaller difference between the area moments of inertial (I) in both major and minor axes of the cross sections with h/b = 1.0, where the effect of ϕ on the reduction factors in the calculation of pre-twisted column strengths is minimised. This would be reflected in the proposed equation for the new reduction factor of the pre-twisted steel columns in Section 5.2 of this paper. However, it should be noted that for the larger ratios of h/b, the optimum ratios of ϕ existed for the ultimate load of the columns, e.g., the ϕ = 90 °/m yielded maximum ultimate load compared with other values of ϕ for the column with h/b = 2.8 and L_e = 4.0 m, as shown in Figure 11b.

4.4 Effects of ϕ with different boundary conditions

The effects of ϕ with different end boundary conditions were investigated for the specimens with the same Section 280×100×10×16 mm with h/b = 2.8 and L_e = 4.0 m (see Table 5c). The pin-end boundary conditions with free rotation about both minor and major axes of the sections were assigned to the specimens. The ultimate loads and failure mode were presented in Table 8. The results in Table 8 were compared with those in Table 6e for the same specimen series. Note that the specimens in Tables 6e had the pin-end boundary conditions with free rotation about minor axis of the un-twisted cross sections. The comparisons were shown in Figure 12. It was found that whether the degree of freedom for rotation about the major axis of the un-twisted section released or not had little effect on the ultimate loads of the pre-twisted steel box-section columns. This may be due to the flexural buckling failure mode about the minor axis at the mid-height dominated the failure of the specimens.

4.5 Effects of ϕ on warping normal stress of the cross sections

For the pre-twisted steel box-section columns under axial loading with pin-end boundary conditions, due to the tilting of the force-bearing fibres across the sections, the axial force will produce bi-moment and torsional moment at sections along the height of the columns. The internal forces including axial compression force, bi-moment and torsional moment could be developed at sections along the height of the columns. The total normal stress produced at the section is the sum of the normal stress due to the axial compression force and the warping normal stress due to the bi-moment. The associated warping normal stress due to the bi-moment moment may affect the mechanical behaviour of the columns. There is limited investigation on the effects of ϕ on the warping stress of the twisted members. Figure 13 illustrates the distributions of warping normal stresses induced by the bi-moment on the box-section of the column. The warping normal stresses equal to zero at the midpoint of the webs and flanges, and maximum warping normal stresses are found at the corner of the cross section. It is shown that the warping normal stresses are in anti-symmetric distribution in the cross section, which indicates that the resultant axial force from the warping normal stress in the cross section equals to zero.

In this study, the specimens in Table 6a (i.e., specimen series 280×100×10×16-1.0) were used to investigate the distribution of the warping normal stress under the axial load of 2000 kN. The warping normal stress was obtained by the difference between the total normal stress and the normal stress due to axial compression force. The maximum warping normal stresses at different cross sections along the longitudinal direction of the columns were shown in Figure 14 for specimen Series 280×100×10×16-1.0. The vertical axis plots the maximum warping normal stress while the horizontal axis shows the location along the height of the column, i.e., in the range of 0.1~0.9 m for L_e = 1.0 m. Hence, the effects of ϕ on the distribution of maximum warping normal stress at sections along the column height were illustrated. It was found that the maximum warping normal stress of the section increased from the section at the mid-height of the column to the section at the column ends in both directions for different values of ϕ. The maximum warping normal stress became larger at the same location for the larger value of ϕ, for example, 16.17 MPa for ϕ = 120 °/m compared with 0.26 MPa for ϕ = 3 °/m at the location of 0.9 m. However, the warping normal stresses of the columns due to the effects of ϕ are quite small compared with the yield stress of the material (see the values of f_y > 235 MPa obtained from coupon tests in Table 2) and even far smaller than the working stress level of 245 MPa under the applied axial load of 2000 kN. This means that the warping normal stresses induced by the pre-twisting of the steel box-section columns are negligible.

4.6 Effects of ϕ on torsional shear stress

Following the above, the maximum torsional shear stresses on the cross sections along the longitudinal direction of the columns were investigated. The maximum torsional shear stress was found at the middle positions of the flanges and webs of the cross sections. The maximum torsional shear stresses of the webs and flanges at the mid-height of the columns were obtained and plotted in Figure 15 for sections 280×100×10×16-1.0 and 280×100×10×16-4.0. It was shown that the maximum torsional shear stress increased with the increment of pre-twisted angle ratio (ϕ), e.g., for the column Series 280×100×10×16-4.0, the maximum torsional shear stress of 45.96 MPa for ϕ = 120 °/m compared with that of 1.04 MPa for ϕ = 3 °/m, as shown in Figure 15. As expected, the results showed that for a given value of ϕ, the effective lengths (L_e) of the column had little effects on the values of maximum torsional shear stress in the pre-twisted columns (see Figure 15). Furthermore, the maximum torsional shear stress at the flanges were much larger than those at the webs, and their differences were larger for the larger value of ϕ. However, the torsional shear stresses of the columns due to the effects of ϕ are small compared with the yield stress of the steel plates (see the values of f_y obtained from coupon tests in Table 2).

4.7 Effects of ϕ on section flexural rigidity

The effects of ϕ on the section flexural rigidity (EI) of the pre-twisted steel box-section column were investigated, where I is the moment of inertia about the minor axis of the un-twisted section. The specimens shown in Tables 6c-6e with section 280×100×10×16 mm and h/b = 2.8 were selected. Three different values of L_e and nine cases of ϕ for the columns were considered, i.e., the values of L_e were 2.0, 3.0 and 4.0 m, and those of ϕ were 0, 3, 10, 15, 20, 30, 60, 90 and 120 °/m.

For the relatively long steel columns without pre-twisting, the overall buckling will occur about the minor axis of the cross section under axial loading condition. It should be noted that the flexural rigidity (EI_{minor}) of the cross section was constant along the column height for columns without pre-twisting. However, for the pre-twisted steel box-section columns, the flexural rigidity (EI) of the cross section was varied along the column height due to the changing of area and distance about the neutral axis of the cross section. For the pre-twisted steel columns, the flexural rigidity (EI) was varied between the minimum of EI_{minor} and the maximum of EI_{major} of the cross section, where I_{major} is the moment of inertia of the section about the major axis. Compared with the section flexural rigidity (EI_{minor}) of the steel columns without pre-twisting that will fail in buckling about the minor axis of the section, the flexural rigidity of the pre-twisting of the sections along the columns are improved, namely, they are larger than EI_{minor}. This means that the pre-twisting improves the overall flexural rigidity (about the minor axis of the un-twisted section) of the columns for the same L_e. Hence, the lateral deformations (about the minor axis) were reduced while the ultimate loads were increased.

Figures 16a-16c show the applied load versus the deflection at the mid-height of the columns for the L_e of 2.0, 3.0 and 4.0 m, respectively. The applied loads were scaled up to 1000 kN. In each figure, the aforementioned nine values of ϕ were included. It was found that the lateral deflections at the mid-height of the columns were smaller for the pre-twisted steel box-section columns than those of columns without pre-twisting. For the columns with same value of L_e, the larger value of ϕ generally yielded less lateral deflections under the same axial loading conditions due to the increased section flexural rigidity with the increment of ϕ for the columns with the same L_e, as discussed previously. However, it should be noted that for the section flexural rigidity of the columns Series 280×100×10×16-4.0, the Specimen 280×100×10×16-4.0ϕ90 performed the best (see Figure 16c), i.e., least lateral deflection under the same loading conditions, which was in accordance with the previously findings (See Figure 9) in Section 4.3 of this paper.

5. Loading capacity of pre-twisted steel box-section column

5.1 Design rules in current specifications

To the authors' knowledge, there are no design rules for the pre-twisted steel box-section columns. Hence, the current international steel design specifications including EC3-1.1 [17], ANSI/AISC 360-16 [18] and GB 50017-2017 [19] for steel members without pre-twisting were used to calculate the nominal loading capacities (P_n) of the pre-twisted steel box-section columns considered in this study.

For the design of steel welded box-section columns, the reduction factor (φ) for the relevant flexural buckling mode about the minor axis of the section should be calculated according to Section 6.3.1.2 in the EC3-1.1 [17], where the imperfection factor equals to 0.49 with the corresponding buckling curve "c" in Table 6.2 of the EC3-1.1 [17]. Similarly, the GB 50017-2017 [19] provides the calculation of the reduction factor (φ) in the Appendix D, where it is termed as buckling coefficient (reduction factor) of column. In the ANSI/AISC 360-16 [18], the design of steel columns is provided in Section E3, where the loading capacity is determined based on the limit state of flexural buckling. The loading capacity of the steel columns calculated by using the ANSI/AISC 360-16 [18] was divided by Af_y in this study, in order to obtain the reduction factor (φ). Hence, the reduction factor (φ) calculated by using different design specifications [17-19] for design of steel box-section columns could be directly compared.

In summary, Equation (1) illustrates the calculation of nominal axial loading capacity (P_n) of a steel box-section column:

$$P_n = \varphi A f_y \tag{1}$$

5.2. Proposed design rules for pre-twisted steel box-section columns

As mentioned before, the current international steel design specifications, including EC3-1.1 [17], ANSI/AISC 360-16 [18] and GB 50017-2017 [19], do not provide design rules for pre-twisted steel box-section columns. In this study, theoretical analysis on the elastic flexural buckling of pre-twisted steel box-section columns was conducted. Efforts were made to develop the new equation that would be consistent with the existing one (See Eq. (1)), where the term of Af_y was retained for pre-twisted steel box-section columns. A formula for the reduction factor (buckling coefficient) was proposed for the pre-twisted steel box-section columns, as described in the following.

Assume that when buckling, the buckling direction of the column has a twist angle θ_0 with the major axis at the mid-height of the column. The twist angle θ between the buckling direction and the major axis of any cross section is $\theta = \theta_0 + \phi z$. Hence, the moment of inertial about the minor axis for any cross section is shown in Equation (2):

$$I = I_x cos^2\theta + I_y sin^2\theta \tag{2}$$

where I_x and I_y are the area moments of inertial of the un-twisted section about the minor and major principal axes (x axis and y axis), respectively; ϕ is the pre-twisted angle ratio; z is the coordinate along axial axis of the column, where the mid-height section has $z=0$. Equation (3) shows the assumed deflection curve of the column with both ends were simply supported:

$$y = a_1 \sin\frac{\pi}{l} z \tag{3}$$

where a_1 is a non-dimensional constant value, l is the effective length of the column.

Hence, the strain energy of the column is given in Equation (4):

$$U = \frac{1}{2}\int_0^l \frac{M^2}{EI} dz = \frac{1}{2}\int_0^l \frac{(EIy'')^2}{EI} dz = \frac{1}{2}\int_0^l EIy''^2 dz \tag{4}$$

Substitute Equations (2)-(3) into Equation (4) yields Equation (5):

$$\begin{aligned} U &= \frac{1}{2}\int_0^l E\left(I_x cos^2\theta + I_y sin^2\theta\right)\left(a_1 \frac{\pi^2}{l^2} sin\frac{\pi z}{l}\right)^2 dz \\ &= \frac{1}{2}\int_0^l E\left(I_x cos^2(\theta_0 + \phi z) + I_y sin^2(\theta_0 + \phi z)\right)\left(a_1 \frac{\pi^2}{l^2} sin\frac{\pi z}{l}\right)^2 dz \\ &= \frac{\pi^2 {a_1}^2}{16\theta'(\pi^2 - \phi^2 l^2)}\left[sin2(\theta_0 + \phi l) - 2\sin(2\theta_0)\right]\left[EI_x\left(\frac{\pi}{l}\right)^4 - EI_y\left(\frac{\pi}{l}\right)^4\right] \\ &\quad + \frac{{a_1}^2 l}{8}\left[EI_x\left(\frac{\pi}{l}\right)^4 + EI_y\left(\frac{\pi}{l}\right)^4\right] \end{aligned} \tag{5}$$

The external work (U_p) done by the applied load P under axial deformation (Δ) is shown in Equation (6):

$$U_p = -P\Delta = -\frac{1}{2} P \int_0^l y'^2 \, dz = -\frac{{a_1}^2 \pi^2 P}{4l} \tag{6}$$

Hence, the total potential energy (E) is derived in Equation (7):

$$E = U + U_p \tag{7}$$

In equilibrium state as expressed in Equation (8), the critical buckling load (P_{cr}) of the pre-twisted steel box-section column was obtained as shown in Equation (9).

$$\frac{dE}{da_1} = \frac{d(\mathrm{U}+U_p)}{da_1} = 0 \tag{8}$$

$$P_{cr} = \frac{1}{2}\left[EI_x\left(\frac{\pi}{l}\right)^2 + EI_y\left(\frac{\pi}{l}\right)^2\right] - \left|\frac{\pi^2 \sin(\phi L_e)}{2\phi l_e(\pi^2 - \phi^2 l^2)}\right| \left|\left[EI_x\left(\frac{\pi}{l}\right)^2 - EI_y\left(\frac{\pi}{l}\right)^2\right]\right| \tag{9}$$

When $\phi = 0$, it is a common column without pre-twisting. The critical buckling load is shown in Equations (10) and (11).

$$\lim_{\phi \to 0} \frac{\pi^2 \sin(\phi l)}{2\phi l(\pi^2 - \phi^2 l^2)} = \frac{1}{2} \tag{10}$$

$$P_{cr} = E\left(\frac{\pi}{l}\right)^2 (I_x \,, I_y)_{min} \tag{11}$$

It is shown that the Equation (11) yields the same result as the Euler buckling load for common column without pre-twisting, which depends on the smaller of the area moment of inertial.

When $\phi \neq 0$, the column is pre-twisted with an angle ratio of ϕ. The critical buckling load is shown in Equations (12)—(14).

$$P_{cr} = \frac{1}{2}\left[P_{crx} + P_{cry}\right] - \left|\frac{\pi^2 \sin(\phi l)}{2\phi l(\pi^2 - \phi^2 l^2)}\right| \left|P_{crx} - P_{cry}\right| \tag{12}$$

$$P_{crx} = \frac{\pi^2 EI_x}{l^2} \tag{13}$$

$$P_{cry} = \frac{\pi^2 EI_y}{l^2} \tag{14}$$

where I_x and I_y are the area moments of inertial of the un-twisted section about the minor and major principal axes (x axis and y axis), respectively. This means that both the area moments of inertial about the minor and major axes have contributions to the pre-twisted steel box-section column capacity depends on the value of pre-twisted angle ratio of ϕ.

With an analogy to the design of a common steel column without pre-twisting, the new reduction factor (φ_P) was further proposed to consider the effects of initial geometric imperfections and residual stresses, as shown in Equation (15). In which φ_x and φ_y are the reduction factors about the x axis and y axis of the original section. The GB 50017-2017 [19] was adopted in this study to calculate the values of φ_x and φ_y for steel box-section column. Hence, the ultimate loads (P_p) of the pre-twisted steel columns with rectangular hollow sections are predicted by using the Equation (16), which could consider the effect of ϕ on the capacity of the pre-twisted steel box-section column.

$$\varphi_p = \frac{1}{2}\left[\varphi_x + \varphi_y\right] - \frac{1}{2}\left|\varphi_x - \varphi_y\right| \left|\frac{\pi^2 \sin(\phi l)}{2\phi l(\pi^2 - \phi^2 l^2)}\right| \tag{15}$$

$$P_p = \varphi_p A f_y \tag{16}$$

6. Comparison of reduction factors

The reduction factors (buckling coefficients) of the columns were calculated by using $\varphi = P/Af_y$. The parametric study results of the 60 specimens in Table 5a were used to calculate the reduction factors (φ_{FEA}) for column series with different effective lengths. The reduction factors calculated from the aforementioned steel design specifications were shown in Figures 17a-17d. In the calculations, the nominal dimensions of the cross section and the material properties of steel plate 10 mm and 16 mm (see Table 2) were used. The terms of φ_{EC3}, φ_{AISC} and φ_{CN} mean the calculated values from the EC3-1.1 [17], ANSI/AISC 360-16 [18] and GB 50017-2017 [19], respectively. It should be noted that the current steel design specifications [17-19] do not provide design rule for the pre-twisted steel columns. Hence, the results for the steel columns without pre-twisting were used for the pre-twisted steel columns. In addition, the proposed Eq. (15) in this study was also used to calculate the reduction factors (φ_P) for the columns.

The reduction factors of φ_{FEA} were compared with those calculated by using the current steel design specifications [17-19], as well as those calculated by the proposed Eq. (15) for the 60 column specimens. The mean values of $\varphi_{FEA}/\varphi_{EC3}$, $\varphi_{FEA}/\varphi_{AISC}$, $\varphi_{FEA}/\varphi_{CN}$ and φ_{FEA}/φ_P are 1.15, 1.01, 1.06 and 0.99, with the corresponding coefficient of variation (COV) of 0.106, 0.054, 0.069 and 0.049. Overall, it is shown the calculated values from the current steel design specifications are conservative, where the calculated values from the EC3-1.1 [17] are the most conservative. The ANSI/AISC 360-16 [18] provides the best calculated values compared with those calculated by using EC3-1.1 [17] and GB 50017-2017 [19], as the mean value of $\varphi_{FEA}/\varphi_{AISC}$ is more close to 1.00 with smaller value of COV 0.054. However, it was shown from the Figures 17a-17d that constant value of reduction factor (φ_{EC3}, φ_{AISC} and φ_{CN}) obtained from the current international steel design specifications [17-19] cannot used to calculate the reduction factor (φ_{FEA}) that obtained from the numerical study, while the calculated reduction factor (φ_p) by using the proposed Eq. (15) can generally match well with the φ_{FEA}, in particular in Figures 17b-17d. Furthermore, it was found that the calculated values by the proposed Eq. (15) were more accurate than those calculated by using the design codes [17-19], with the smallest value of COV of 0.049. However, it should be noted that the noted that the reliability of the proposed Eq. (15) is unknown for the pre-twisted angle ratio larger than 15 degree/m (i.e., ϕ > 15 °/m) since the FEA results for this range are not sufficiently validated as discussed in Section 3.2.

7. Conclusions

This paper firstly presented a series of column tests conducted on pre-twisted steel box-sections. The box-sections were fabricated by welding the pre-deformed heat-treated structural steel plates. The grades of steel plates were Q235 and Q345 with the nominal yield stresses of 235 MPa and 345 MPa, respectively. Six pre-twisted steel box-section columns were designed that covering different steel grades, column effective lengths (L_e), pre-twisted angle ratios (ϕ), section dimensions and slenderness (λ).

Secondly, a non-linear finite element model (FEM) was developed and verified against the test results in terms of ultimate loads, failure modes and load-deformation curves. After successful verification, the FEM was employed to conduct an extensive parametric study on the structural behaviour of pre-twisted steel box-section columns. The key parameters in the parametric study included the pre-twisted angle ratios (ϕ), ratios of section depth to width (h/b), effective column lengths (L_e) and end boundary conditions. Findings from the experimental investigation and numerical analysis are summarized in the following:

- It was found that the ϕ has little effect on the ultimate load and initial stiffness of short columns.
- For the long pre-twisted columns failed in flexural buckling, the larger ϕ generally yielded larger ultimate loads due to the improved section flexural rigidity (EI) along the column length as compared with that of columns without pre-twisting. However, the optimum ratios of ϕ existed for the largest ultimate loads among long pre-twisted columns.
- The warping normal stress and shear stress of the columns due to the effects of ϕ

were small compared with the yield stress of the material, and had negligible effects on the ultimate loads of the pre-twisted steel box-section columns.

- Generally, the pre-twisting improved the section flexural rigidity (*EI*) of the box-section column. Hence, the lateral deformations at the mid-height of the columns were reduced while the ultimate loads were increased.

Lastly, theoretical analysis on the elastic flexural buckling of pre-twisted steel box-section columns was conducted. A formula for the reduction factor (buckling coefficient) was proposed. The reduction factors calculated by using the formula, and those calculated by using the European Code [17], American Specification [18] and Chinese Standard [19] for the design of steel structures were compared with those obtained from the parametric study for pre-twisted steel box-section columns.

- Overall, it was shown that the calculated values from the current steel design specifications were conservative. Specially, the calculated values from the EC3-1.1 [17] were found the most conservative while the ANSI/AISC 360-16 [18] provided the most accurate calculated values.
- It was found that the calculated values by using the proposed formula generally were more accurate than those calculated by the current design specifications [17-19].
- The proposed formula in this study is suitable for the prediction of ultimate strengths of pre-twisted steel box-section columns without the failure of local buckling, where the steel columns satisfy the limits of $\phi \leq 120$ °/m, $h/b = 2.8$ and $L_e \leq 4.0$ m. However, it should be noted that the reliability of the proposed formula for the pre-twisted angle ratio larger than 15 degree/m (i.e., $\phi > 15$ °/m) need be further investigated since the FEA results for this range are not sufficiently validated.

Acknowledgements

The research work described in this paper was supported by research grants from the State Key Laboratory for Disaster Prevention in Civil Engineering (Grant No.: SLDRCE19-B-07). The second author would also like to acknowledge the travel grant for academic visit awarded by China Affair Office at The University of Hong Kong.

References

[1] A. Rosen, Structural and dynamic behavior of pretwisted rods and beams, Appl. Mech. Rev. 44 (12) (1991): 483–515.

[2] E. Ghafari and J. Rezaeepazhand, Isogeometric-based cross-sectional analysis of pre-twisted composite beams, Thin-Walled Structures 146 (2020): 106424.

[3] V. Giavotto, M. Borri, P. Mantegazza, G. Ghiringhelli, V. Carmaschi, G.C. Maffioli, F. Mussi, Anisotropic beam theory and applications, Comput. Struct. 16 (1–4) (1983) 403–413.

[4] S. Sina, H. Haddadpour, Axial–torsional vibrations of rotating pretwisted thin walled composite beams, Int. J. Mech. Sci. 80 (2014) 93–101.

[5] M. Borri, G.L. Ghiringhelli, T. Merlini, Linear analysis of naturally curved and twisted anisotropic beams, Compos. Eng. 2 (5–7) (1992) 433–456.

[6] T. Paul and Nivin Philip, Influence of pretwisting angle on the buckling capacity of steel columns: a review, International Journal of Civil Engineering (IJCE) 5(6) (2016): 1-10

[7] S. A. Barakat, F. H. Abed. Experimental Investigation of the Axial Capacity of Inelastically Pretwisted Steel Bars. Journal of Engineering Mechanics, 136(8) (2010): 1028-1035.

[8] W. Fischer. Buckling load of pretwisted rods on knife edge supports. Arch. Appl. Mech, 1970, 39: 28-36.

[9] R. Frisch-Fay. Buckling of pre-twisted bars. International Journal of Mechanical Sciences, 1973; 15(2): 171–181.

[10] B. Tabarrok, Y. Xiong, D. Steinman and W.L. Cleghorn. On Buckling of Pretwisted Columns, International Journal of Solid Structures, 26(5) (1990): 59-72.

[11] M. Serra. Flexural buckling of pretwisted columns. Journal of engineering mechanics, 1993; 119(6): 1286-1292.

[12] D.A. Steinman, B. Tabarrok and W.L. Cleghorn. The effect of pretwisting on the buckling behaviour of slender columns. Int J Mech Sci 1991;33:249–62

[13] Z. Celep. Dynamic Stability of Pretwisted Columns under Periodic Axial Loads, Journal of Sound and Vibration, 103(1) (1985): 35-42.

[14] S. A. Barakat and F. H. Abed. Experimental Investigation of the Axial Capacity of Inelastically Pretwisted Steel Bars. Journal of Engineering Mechanics, 136(8) (2010): 1028-1035.

[15] F. H. Abed, M. H. AlHamaydeh and S. A. Barakat. Nonlinear Finite-Element Analysis of Buckling Capacity of Pretwisted Steel Bars. Journal of Engineering Mechanics, 139(7) (2013): 791-801.

[16] F. H. Abed, M. Megahed and A. Al-Rahmani. On the Improvement of Buckling of Pretwisted Universal Steel Columns, Structures, 5 (2016): 152-160.

[17] EC3-1.1. Eurocode 3: Design of steel structures: Part 1–1: General rules and rules for buildings. BS EN 1993-1-1. London: BSI; 2005.

[18] ANSI/AISC 360-16. Specification for Structural Steel Buildings. ANSI/AISC 360-16, American Institution of Steel Construction, Chicago IL, USA, 2016.

[19] GB 50017-2017. Code for design of steel structures. Beijing: China Architecture & Building Press; 2017 [in Chinese].

[20] GB/T 2975-1998 Steel and steel products: location and preparation of test pieces for mechanical testing. Beijing: China Standard Press; 1998 [in Chinese].

[21] GB/T 228-2002 metallic materials: tensile testing at ambient temperature. Beijing: China Standard Press; 2002 [in Chinese].

[22] ABAQUS. ABAQUS/ Standard User's Manual Volumes I-III and ABAQUS CAE Manual. Version 6.4. Hibbitt, Karlsson & Sorensen, Inc. Pawtucket, USA. 2012.

[23] Y. Cai, and B. Young, Bearing factors of cold-formed stainless steel double shear bolted connections at elevated temperatures, Thin-walled Structures, 2016, Vol. 9. 212-219.

[24] H. Li, P. Cao, F. Wei, Effect of ultimate stability capacity of steel boxing column with residual stress and induced bending, Journal of Sichuan Building Science, 2008, 34(3), 30-33. (in Chinese)

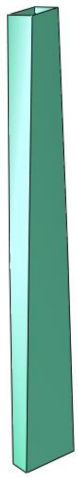

Figure 1: Pre-twisted steel box-section column

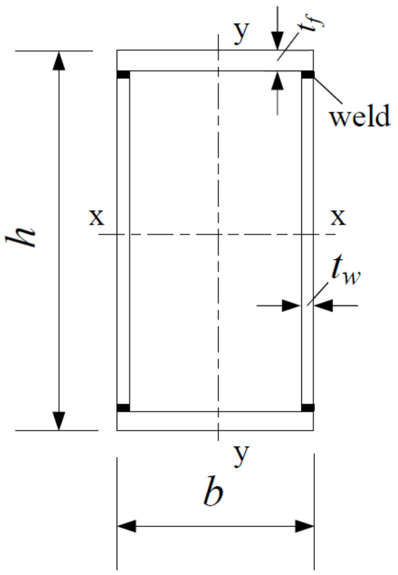

Figure 2: Symbols of a cross section

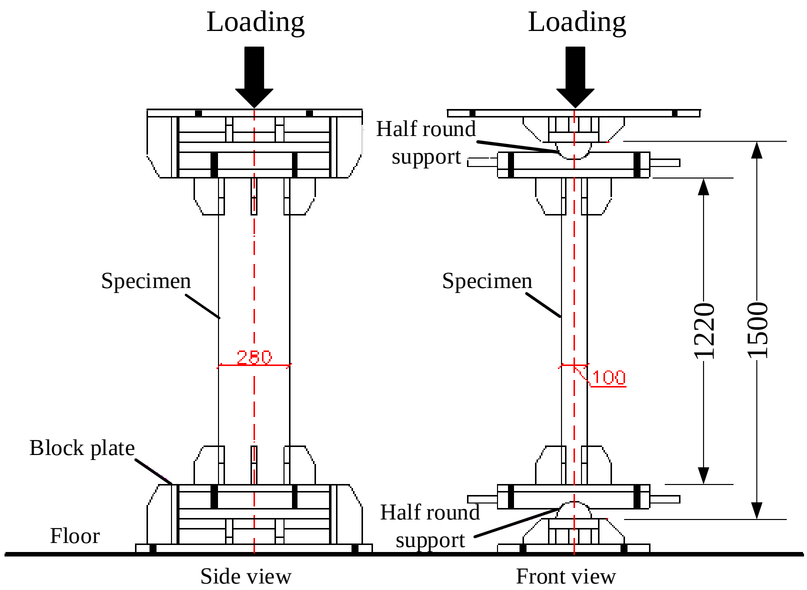

(a) Short column

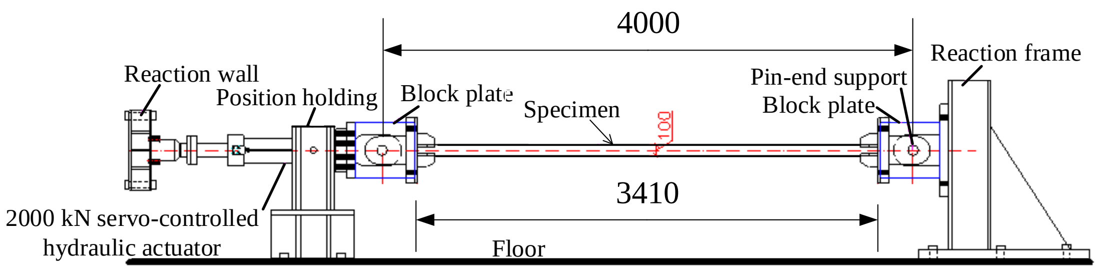

(b) Long column

Figure 3: Schematic view of test setup for steel columns

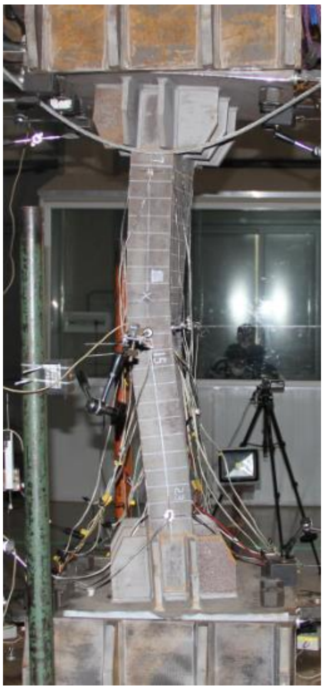

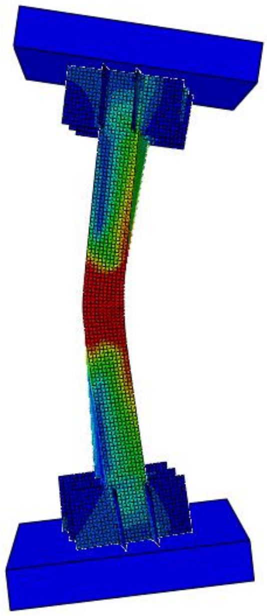

(a) Failure in test (b) Failure in FEA

Figure 4: Comparison of test and numerical failure mode for Specimen 350×120×12×20-1.5-ϕ3

(a) Failure in test

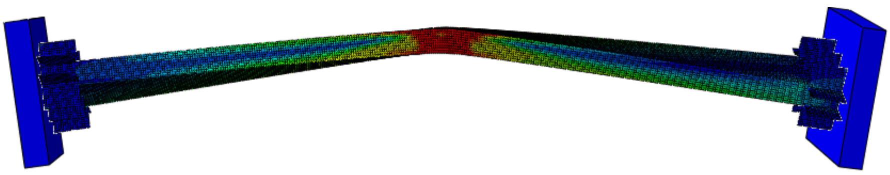

(b) Failure in FEA

Figure 5: Comparison of test and numerical failure mode for Specimen 280×100×10×16-4.0-ϕ15

847

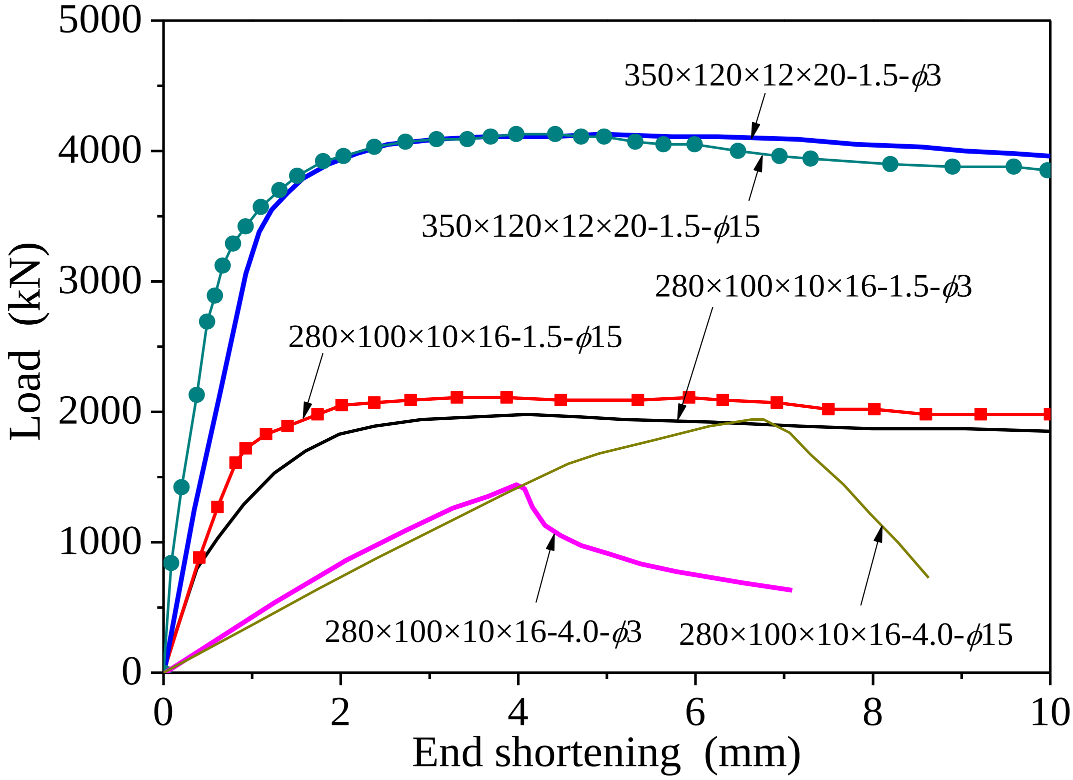

848 **Figure 6:** Load-end shortening curves of tested specimens

849

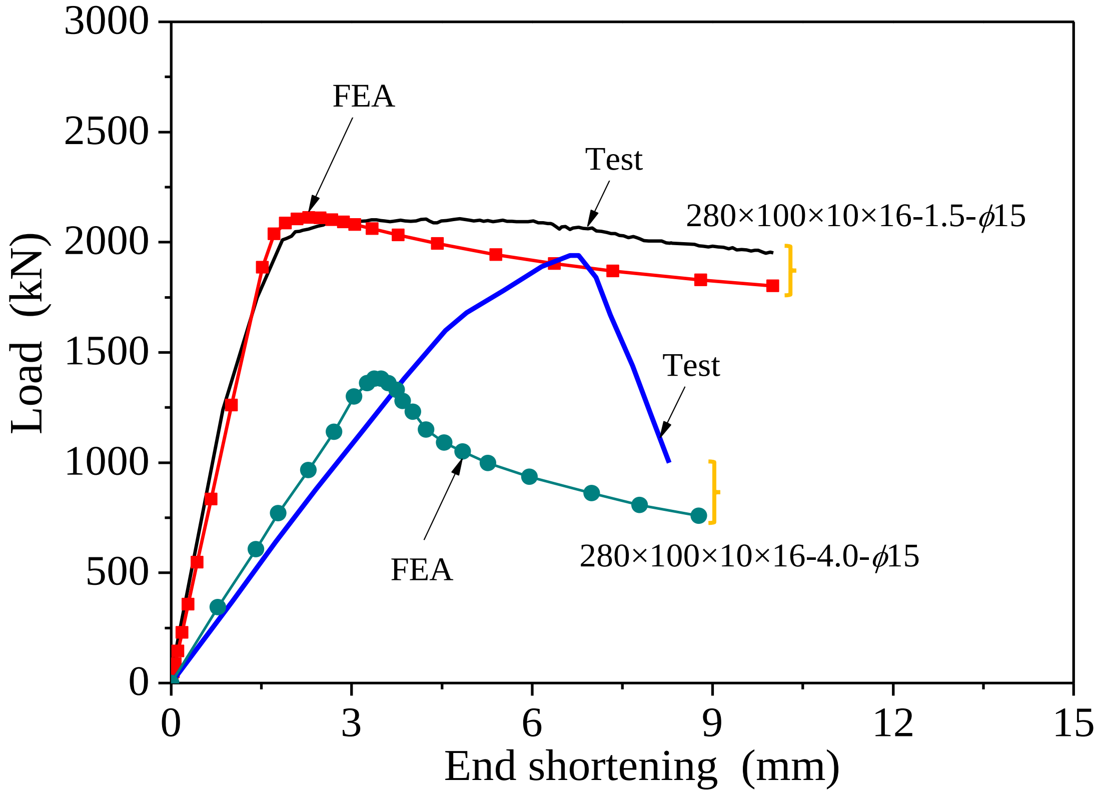

850

851 (a) Comparison of load-end shortening curves obtained from tests and FEA

852

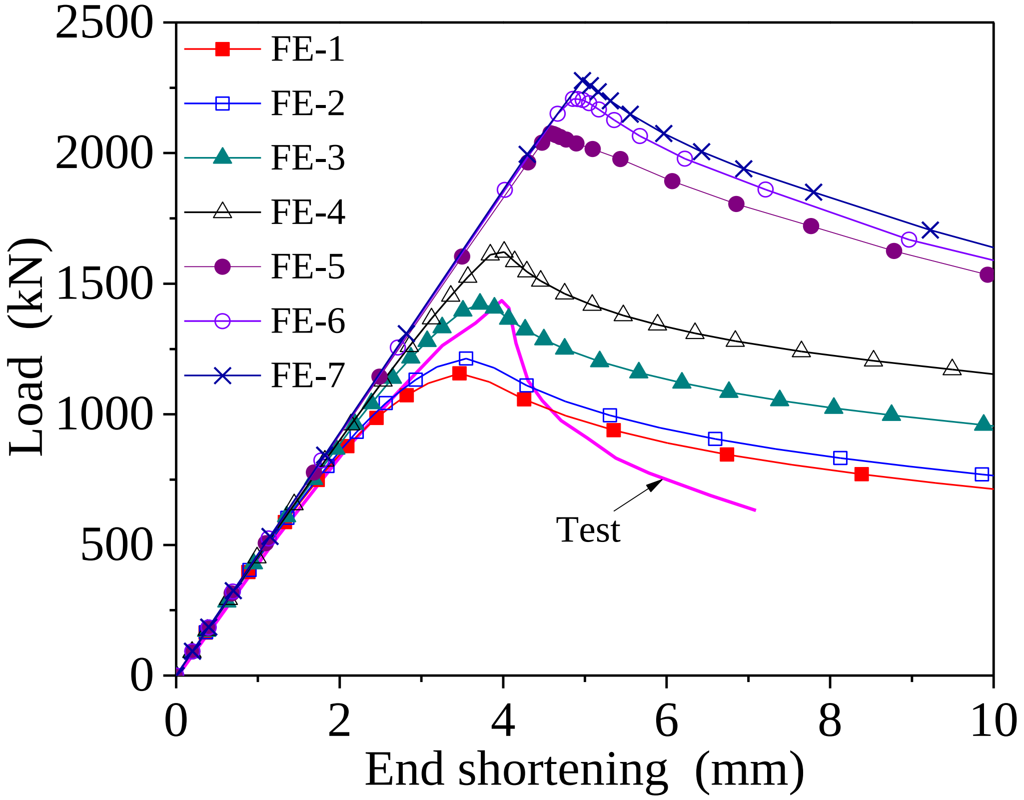

(b) Effects of boundary conditions on the behaviour of specimen 280×100×10×16-4.0-ϕ3

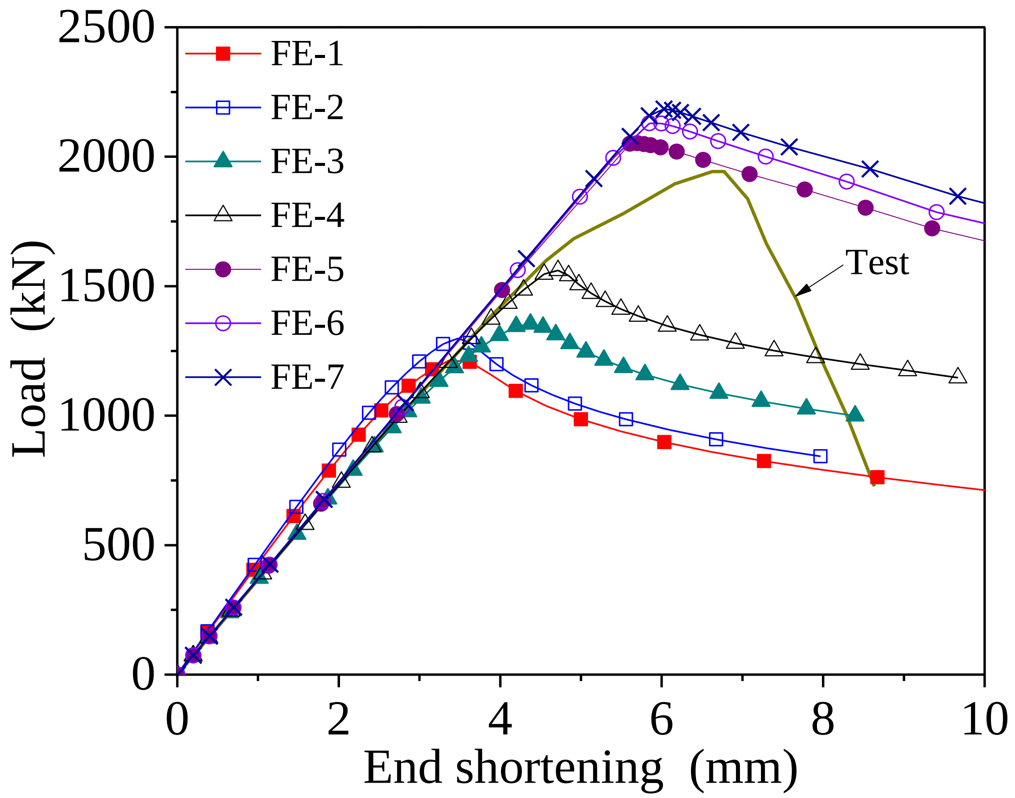

(c) Effects of boundary conditions on the behaviour of specimen 280×100×10×16-4.0-ϕ*15*

Figure 7: Investigation of load-end shortening curves obtained from FEA

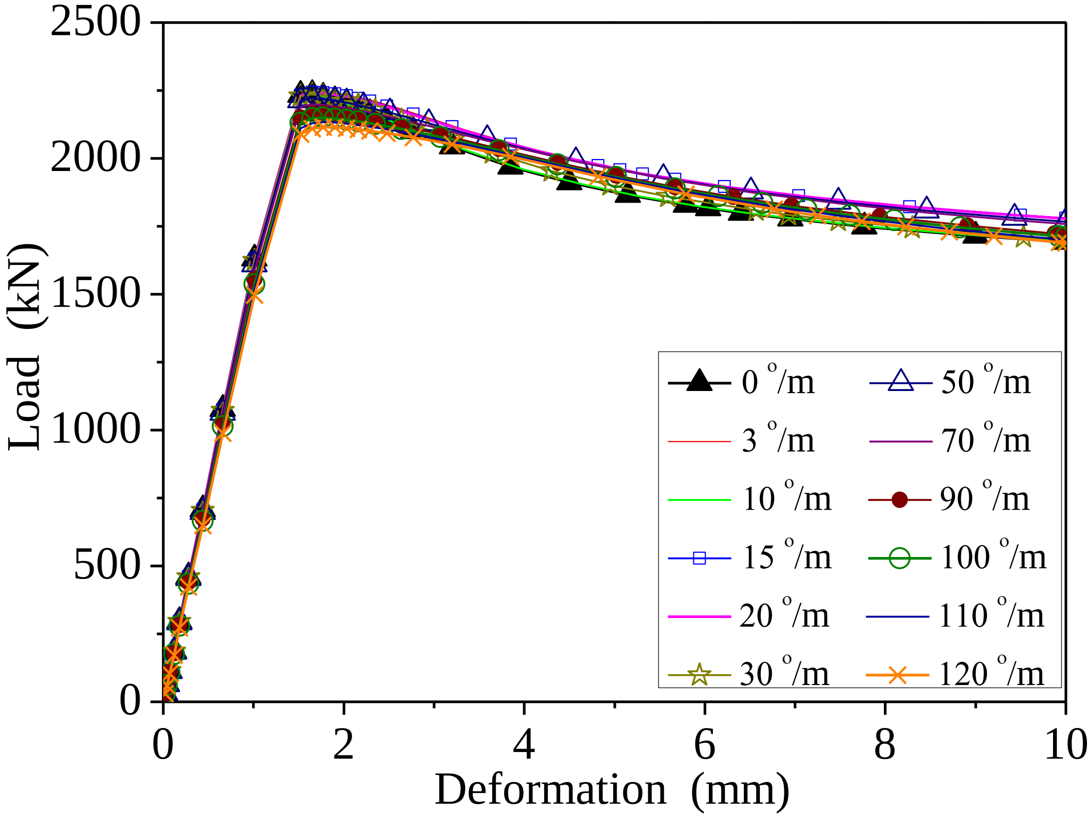

a) L_e = 1.0 m

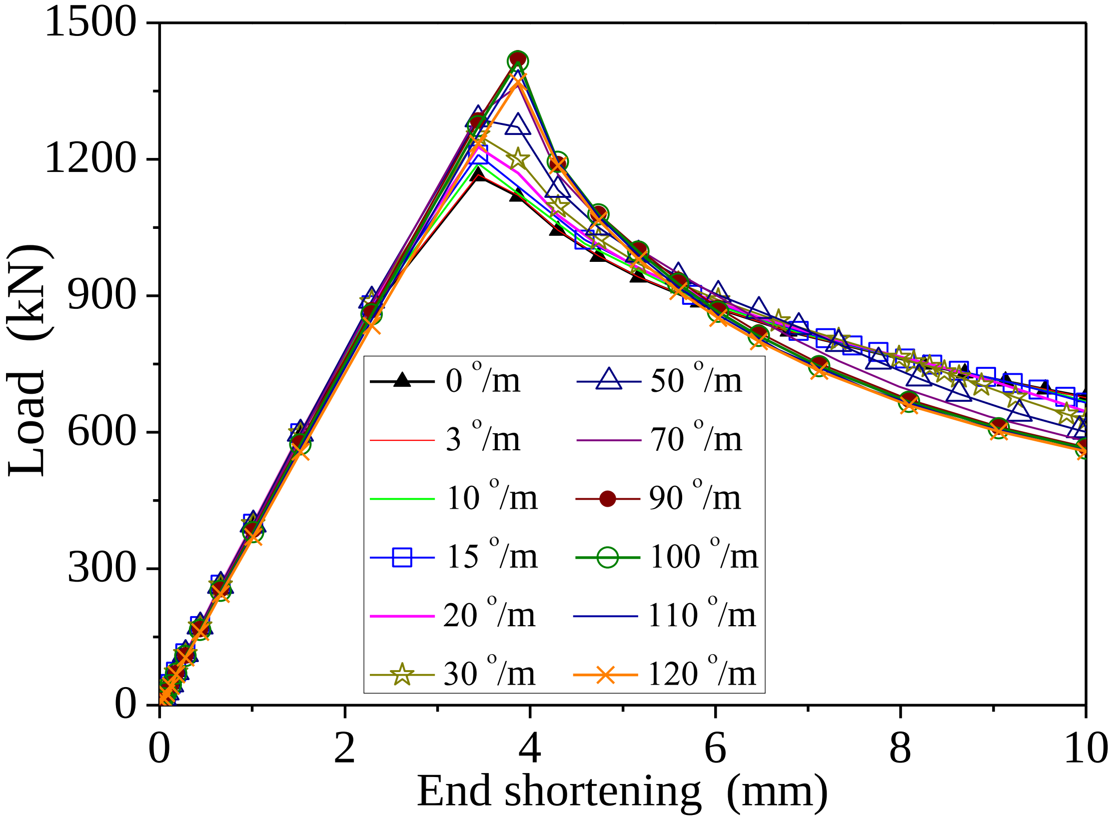

b) L_e = 4.0 m

Figure 8: Load-end shortening curves for specimens with Section 280×100×10×16 mm

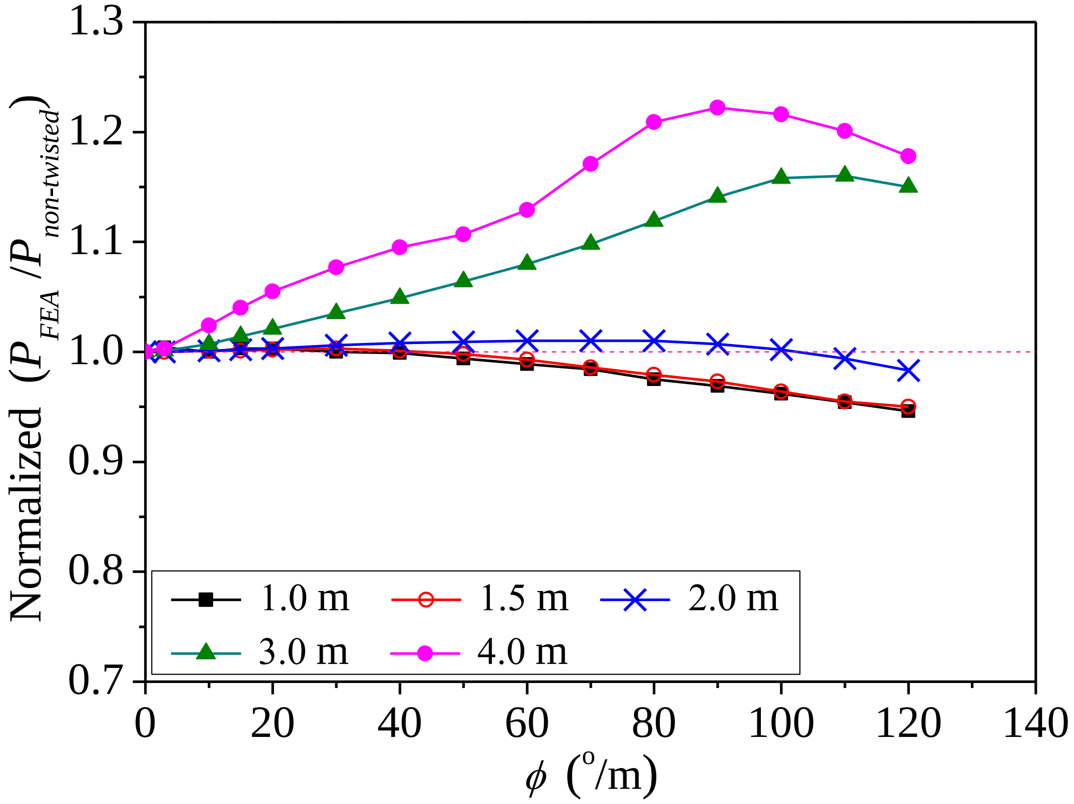

Figure 9: Effects of ϕ on the ultimate loads of columns for Section 280×100×10×16 mm with different L_e

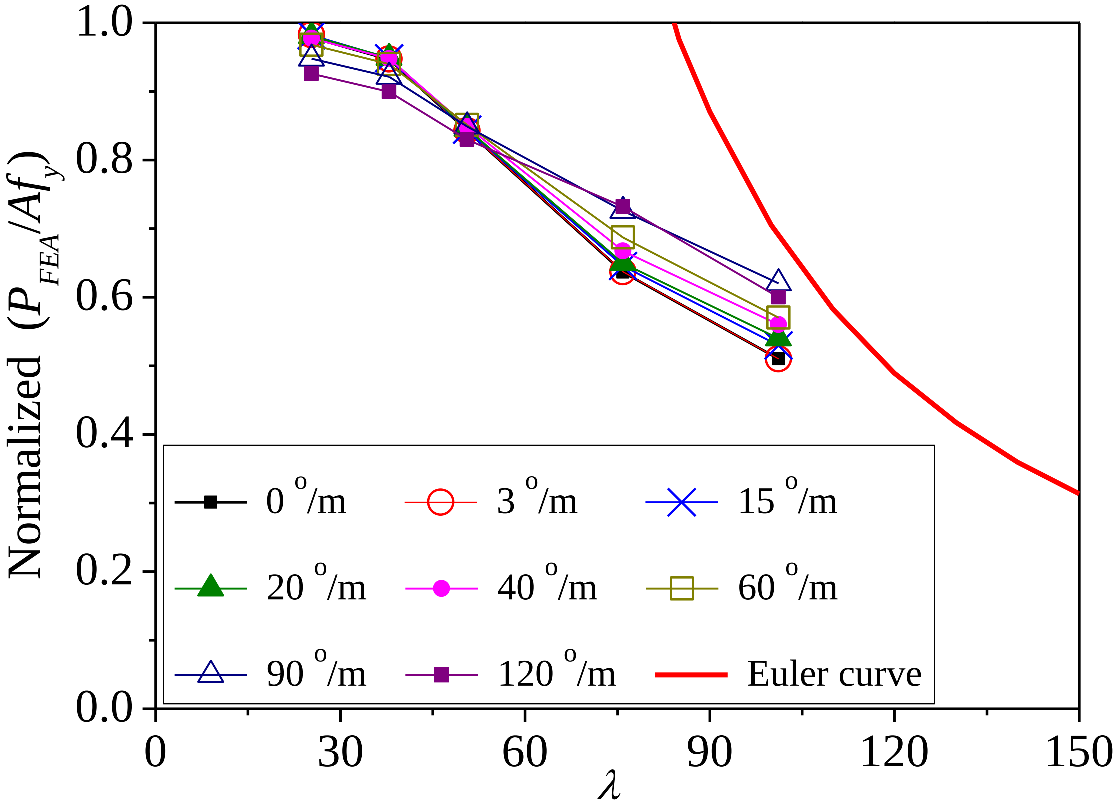

Figure 10: Effects of ϕ on the ultimate loads of columns for Section 280×100×10×16 mm with different member slenderness ratios

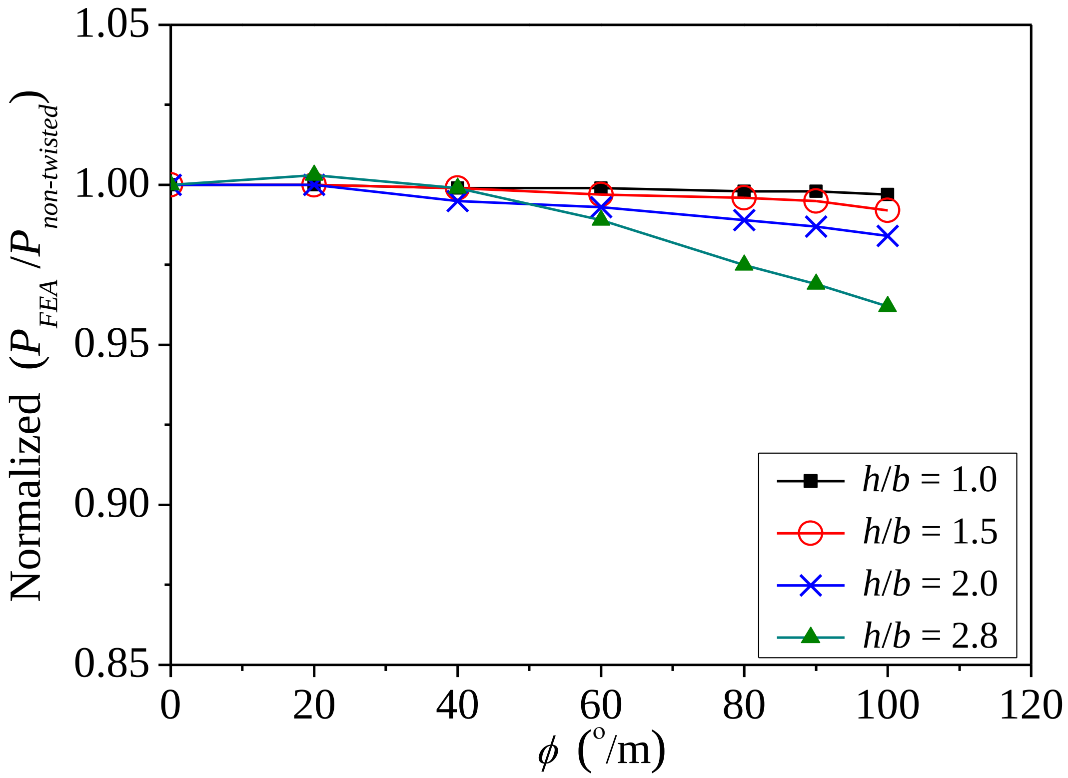

a) L_e = 1.0 m

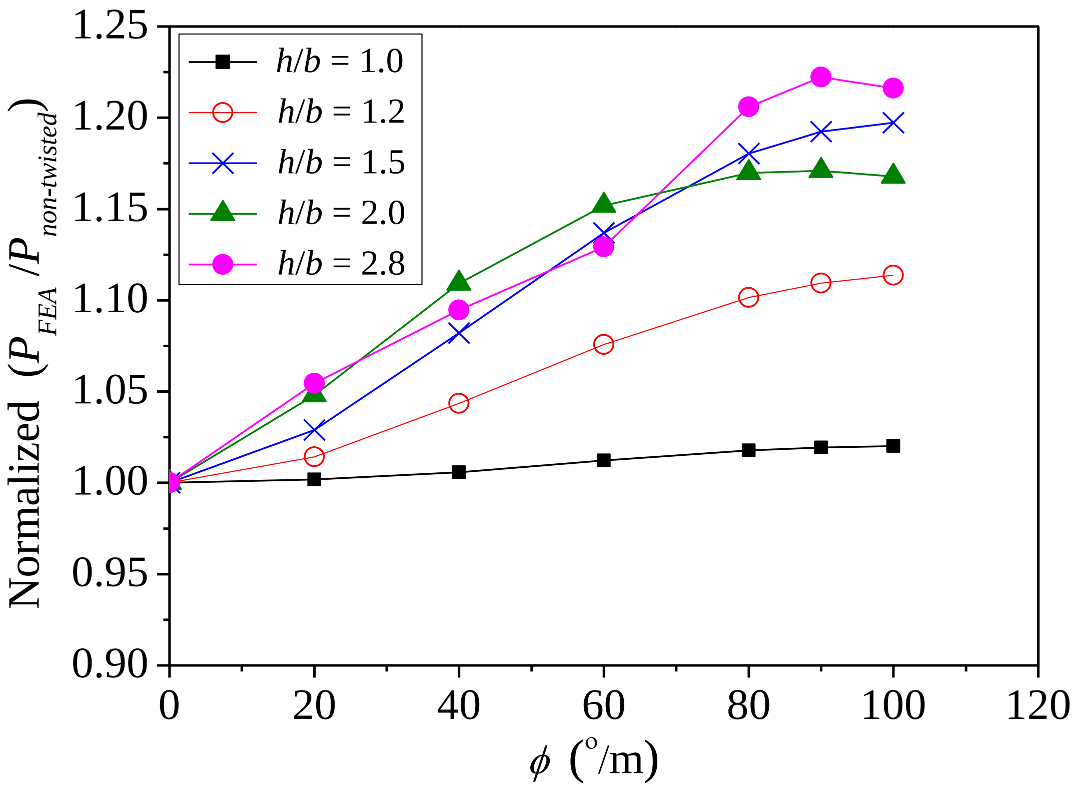

b) L_e = 4.0 m

Figure 11: Effects of ϕ on the ultimate loads of columns for sections with different ratios of h/t

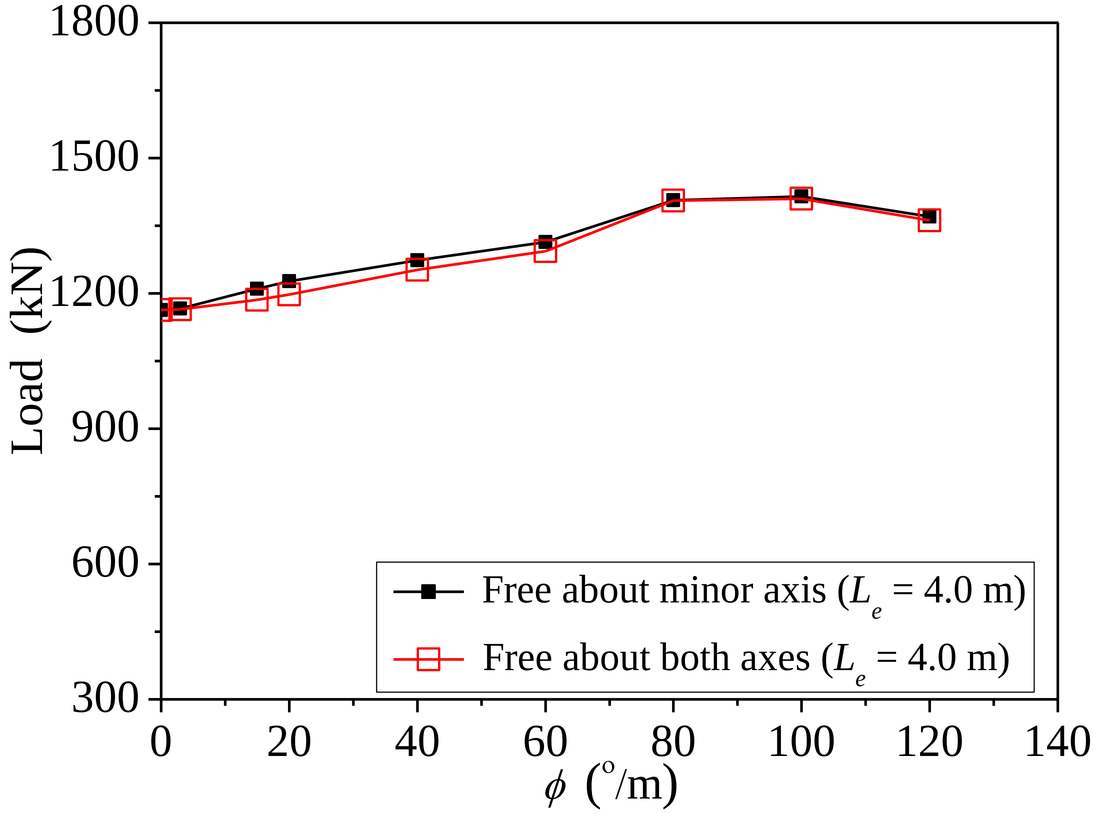

Figure 12: Effects of ϕ on the ultimate loads of columns for Section 280×100×10×16 with different boundary conditions

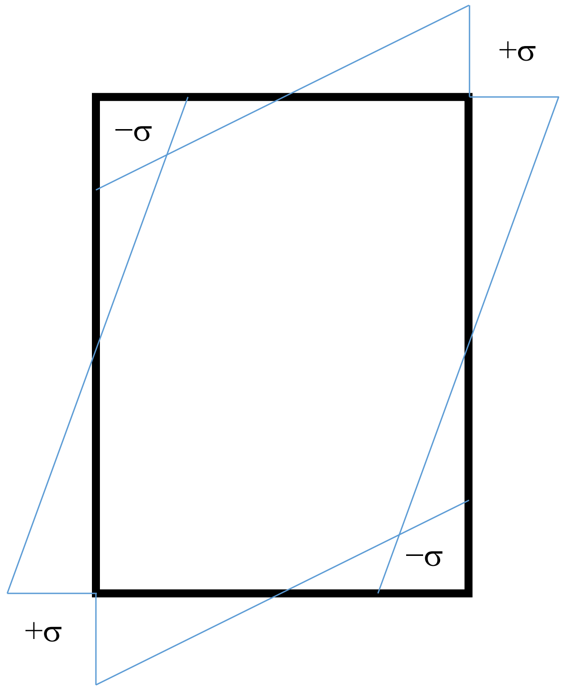

Figure 13: Distributions of warping normal stresses on box-section

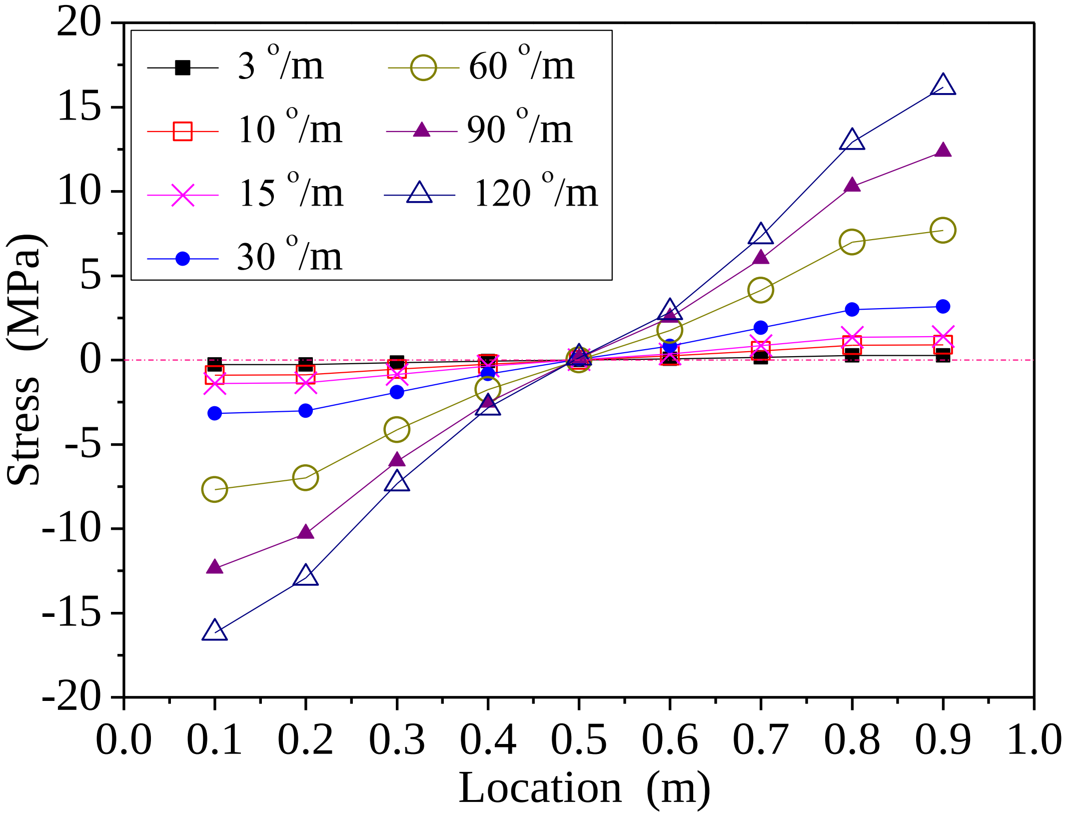

Figure 14: Effects of ϕ on the distribution of maximum warping normal stress at sections along the longitudinal direction of columns for Series 280×100×10×16-1.0

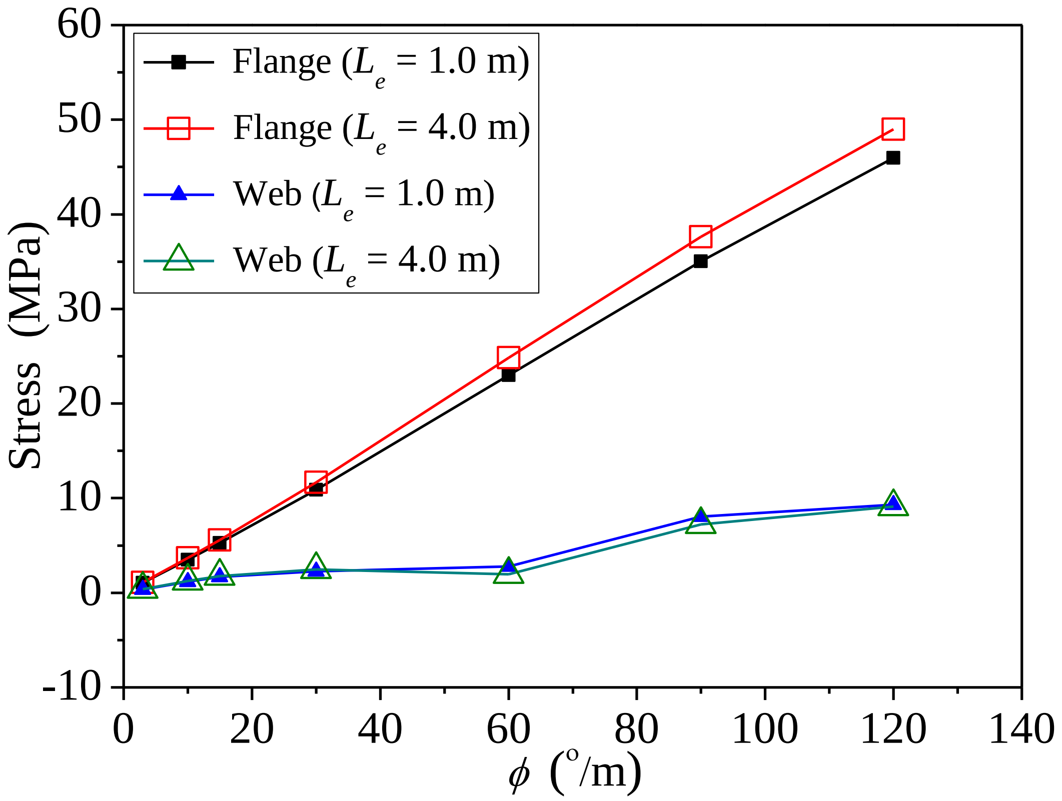

Figure 15: Effects of ϕ on maximum torsional shear stress in the section of columns for Section 280×100×10×16 mm

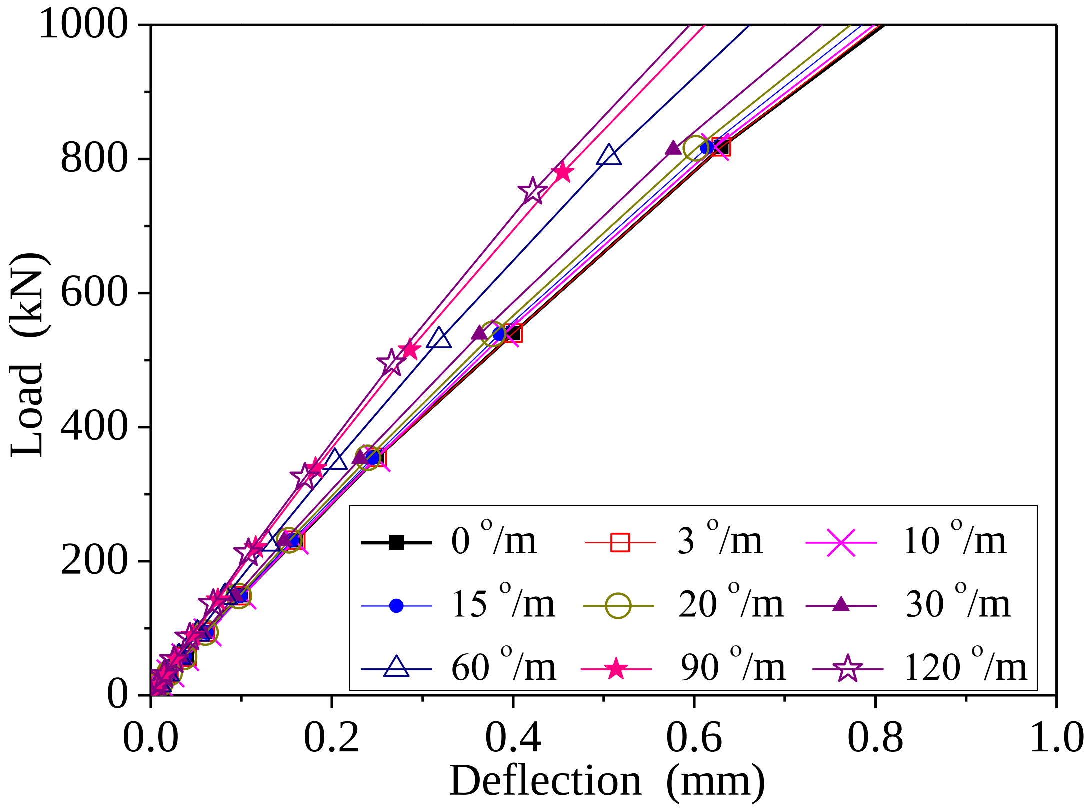

a) L_e = 2.0 m

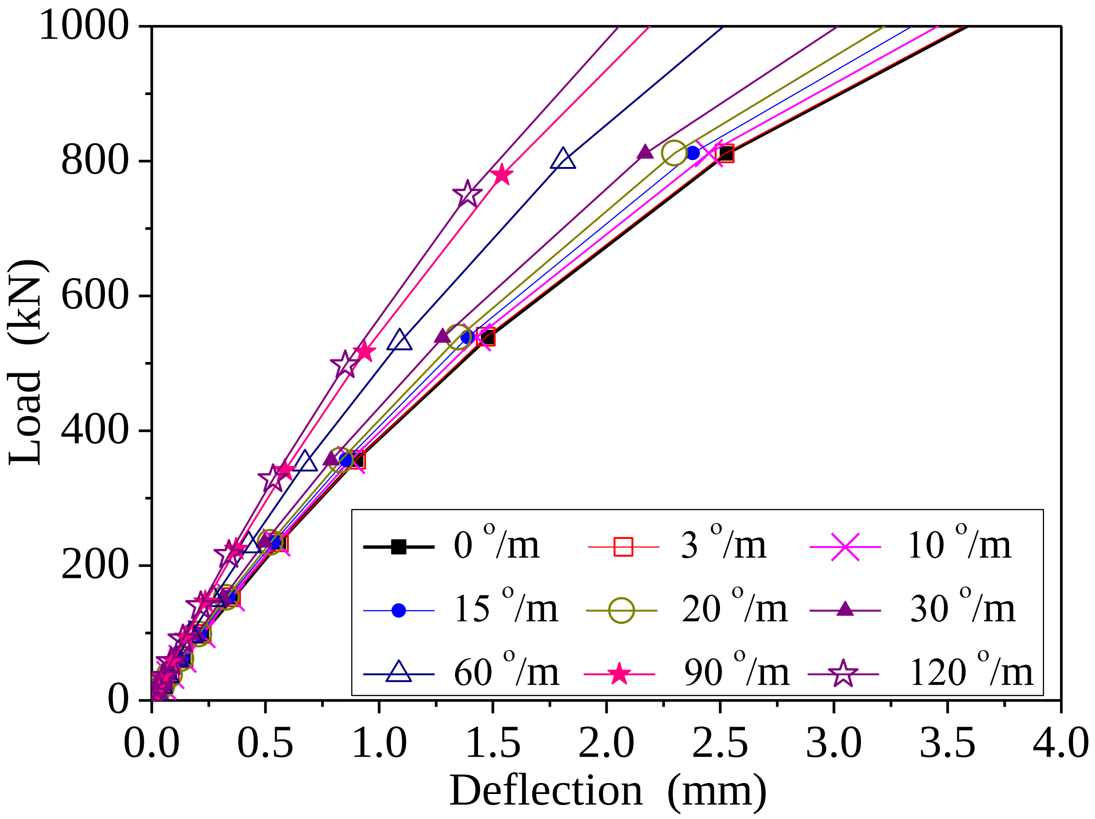

b) L_e = 3.0 m

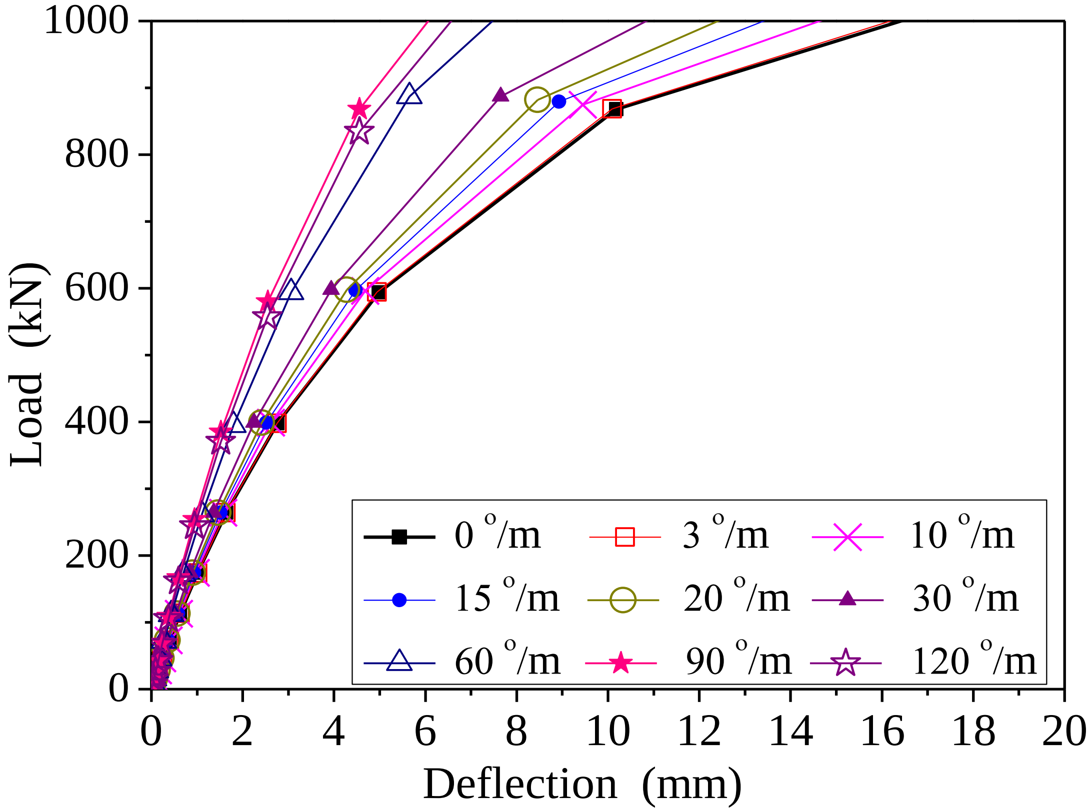

c) L_e = 4.0 m

Figure 16: Load-lateral deflection curves at mid-length of column specimens with different ϕ for Section 280×100×10×16

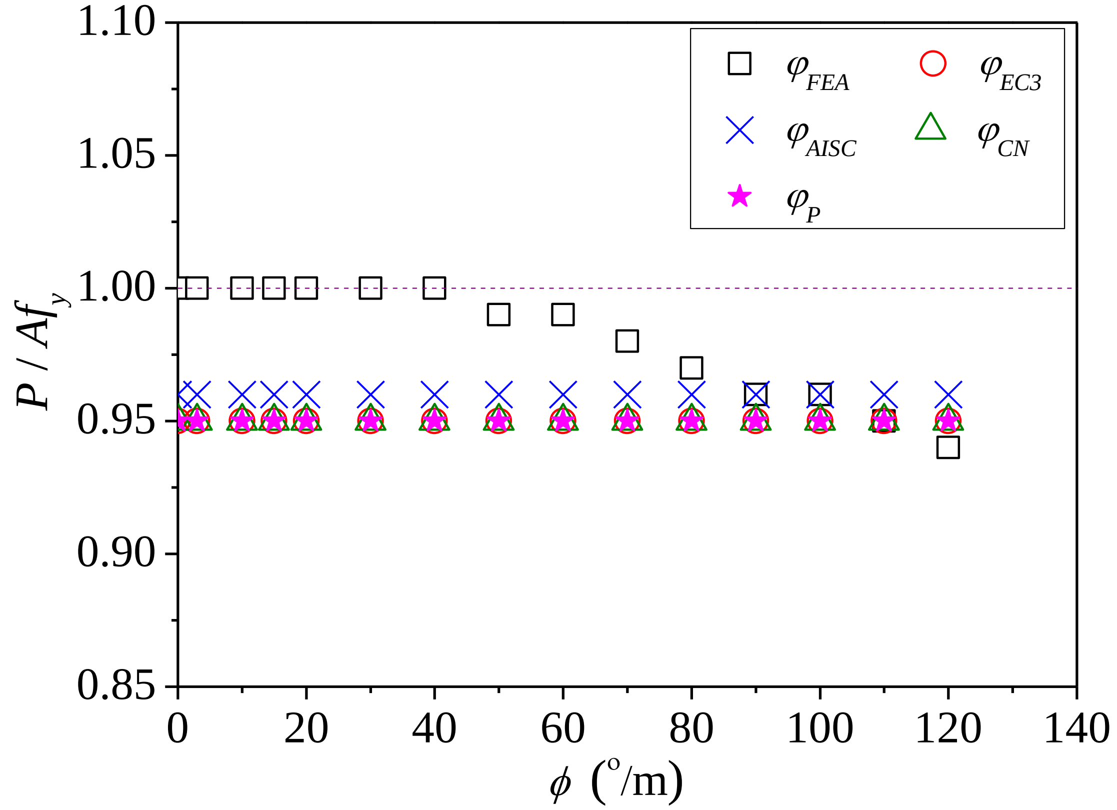

a) L_e = 1.0 m

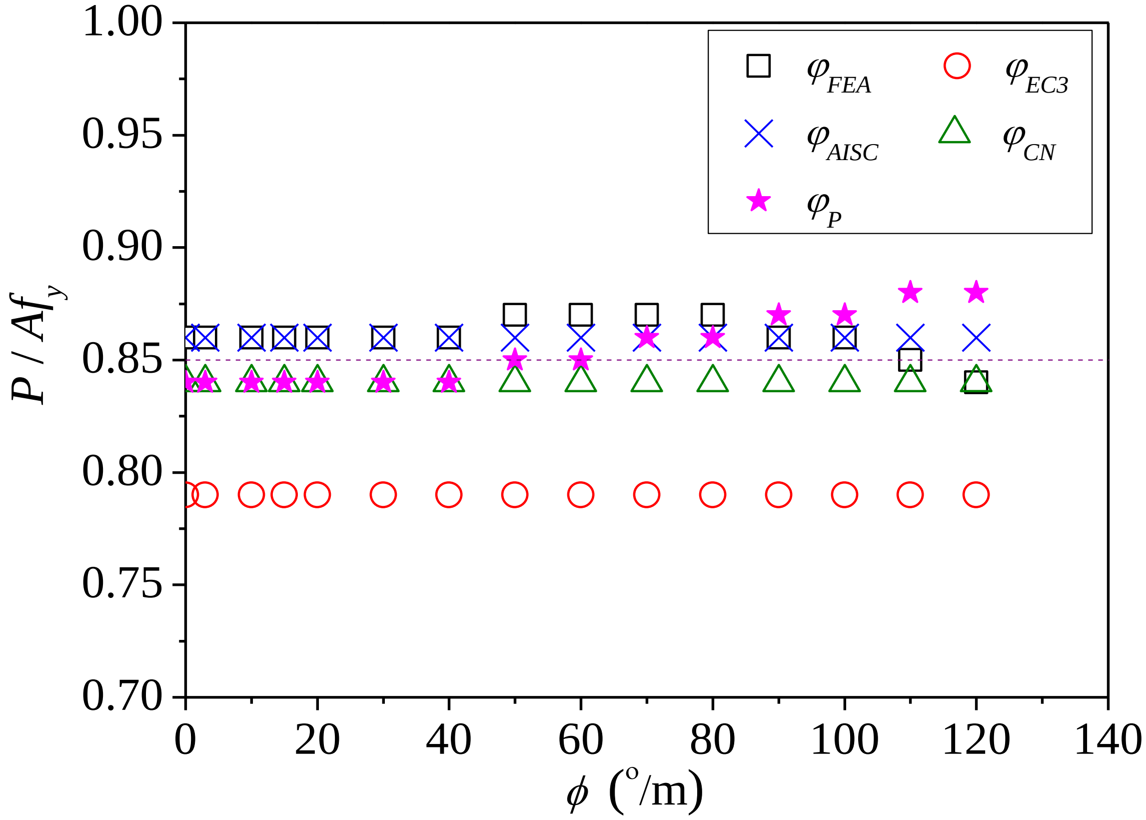

b) L_e = 2.0 m

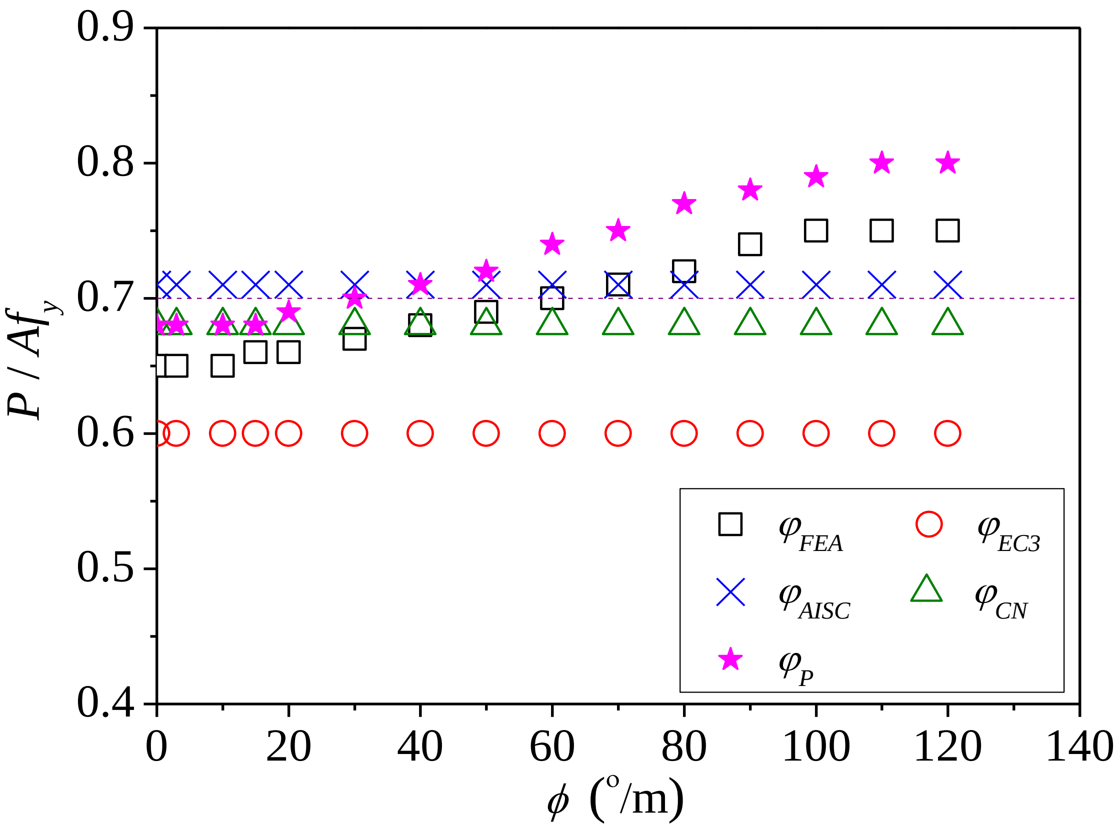

c) L_e = 3.0 m

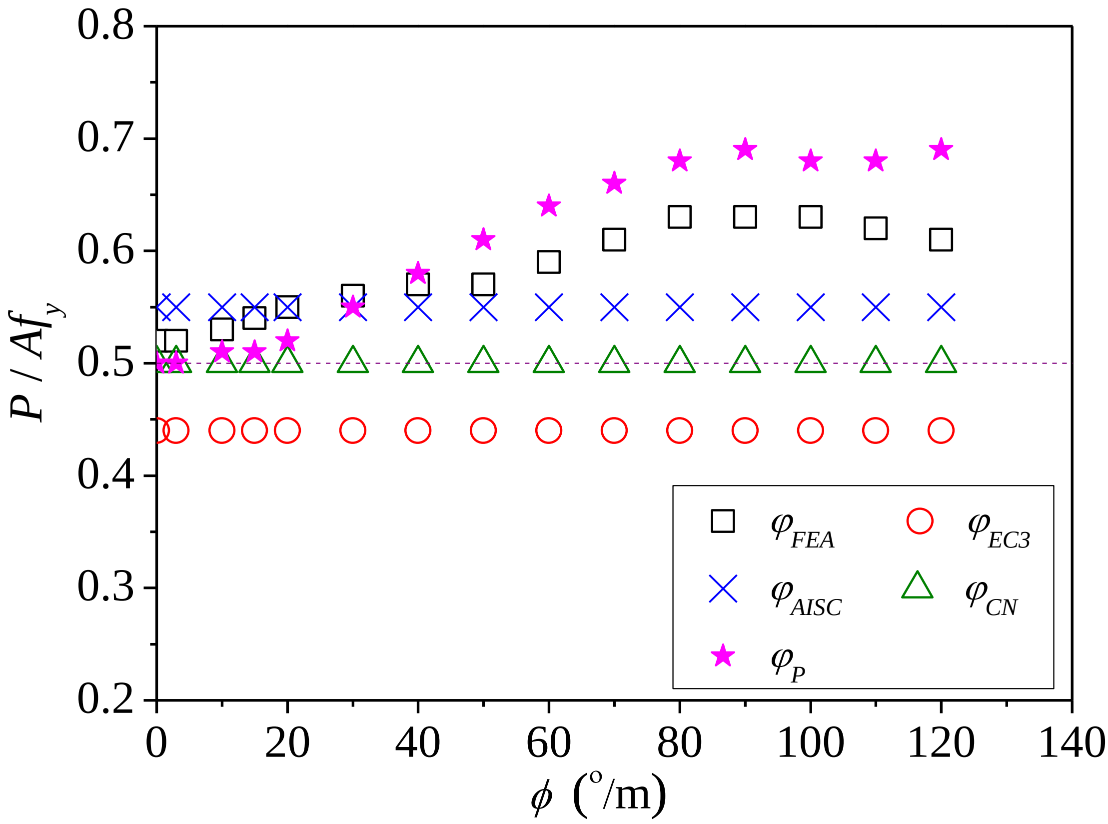

d) L_e = 4.0 m

Figure 17: Comparison of reduction factors for columns with Section 280×100×10×16

Table 1: Dimensions of pre-twisted steel box-section columns

Specimens	Steel grade	h (mm)	b (mm)	t_w (mm)	t_f (mm)	L (mm)	ϕ (°/m)
280×100×10×16-1.5-ϕ3	Q235	280	100	10	16	1220	3
280×100×10×16-1.5-ϕ15	Q235	280	100	10	16	1220	15
350×120×12×20-1.5-ϕ3	Q345	350	120	12	20	1220	3
350×120×12×20-1.5-ϕ15	Q345	350	120	12	20	1220	15
280×100×10×16-4.0-ϕ3	Q235	280	100	10	16	3410	3
280×100×10×16-4.0-ϕ15	Q235	280	100	10	16	3410	15

Table 2: Material properties of steel sheets

Thickness (mm)	E (GPa)	f_y (MPa)	f_u (MPa)	ε_u (%)	ε_f (%)
10	196	284.9	440.0	23.3	33.1
12	195	382.6	534.3	19.5	26.6
16	196	272.1	433.2	24.3	38.3
20	197	344.0	547.2	18.3	29.9

Table 3: Test results of pre-twisted steel box-section columns

Specimen labelling	Test		Section yielding	Failure mode
	P_t (kN)	δ_t (mm)	P_y (kN)	
280×100×10×16-1.5-ϕ3	1971	4.10	2039	Plastic yielding
280×100×10×16-1.5-ϕ15	2105	3.87	2039	Plastic yielding
350×120×12×20-1.5-ϕ3	4120	4.94	4050	Plastic yielding
350×120×12×20-1.5-ϕ15	4156	4.42	4050	Plastic yielding
280×100×10×16-4.0-ϕ3	1436	3.98	2039	Flexure buckling
280×100×10×16-4.0-ϕ15	2000	6.77	2039	Flexure buckling

Table 4(a): Comparison of test and numerical results for pre-twisted steel members

Specimen labelling	Fabrication	Failure mode	P_t (kN)	P_{FEA} (kN)	P_t/P_{FEA}
280×100×10×16-1.5-ϕ3	Steel box-section pre-twisted in factory	Yielding	1971.0	2088.0	0.94
280×100×10×16-1.5-ϕ15			2105.0	2088.0	1.01
350×120×12×20-1.5-ϕ3			4120.0	4277.0	0.96
350×120×12×20-1.5-ϕ15			4156.0	4230.0	0.98
280×100×10×16-4.0-ϕ3		Flexure buckling	1436.0	1167.0	1.23*
280×100×10×16-4.0-ϕ15			2000.0	1210.0	1.65*
				Mean	0.97
				COV	0.028

Note: "*" not included in the comparison.

Table 4 (b): Effects of boundary conditions on the ultimate loads pre-twisted steel members

Cases	Boundary conditions	280×100×10×16-4.0-ϕ3		280×100×10×16-4.0-ϕ15	
	Spring stiffness (N.m/rad)	P_{FEA} (kN)	P_t/P_{FEA}	P_{FEA} (kN)	P_t/P_{FEA}
FE-1	0	1167	1.23	1210	1.65
FE-2	0.1×10^6	1213	1.18	1299	1.54
FE-3	0.5×10^6	1422	1.01	1354	1.48
FE-4	1×10^6	1621	0.89	1561	1.28
FE-5	5×10^6	2076	0.69	2052	0.97
FE-6	10×10^6	2207	0.65	2129	0.94
FE-7	∞	2277	0.63	2185	0.92

Table 5: Key parameters on the structural behaviour of pre-twisted steel columns

(a) Investigation on the effects of ϕ with different L_e

Section	L_e (m)	ϕ (°/m)
280×100×10×16	1.0	0, 3, 10, 15, 20, 30, 40, 50, 60, 70, 80, 90, 100, 110, 120
	1.5	
	2.0	
	3.0	
	4.0	

(b) Investigation on the effects of ϕ with different h/t

Section	h/t	L_e (m)	ϕ (°/m)
100×100×10×16	1.0	1.0, 4.0	0, 20, 40, 60, 80, 90, 100
120×100×10×16*	1.2		
150×100×10×16	1.2		
200×100×10×16	2.0		
280×100×10×16	2.8		

Note: "*" investigated with effective length of 4.0 m.

(c) Investigation on the effects of ϕ with different boundary conditions

Section	L_e (m)	Degree of freedom in rotation	ϕ (°/m)
280×100×10×16	4.0	Free about minor axis;	0, 3, 15, 20, 40, 60, 80, 100, 120
		Free about both major and minor axes	

Table 6: Effects of ϕ on column behaviour for Section 280×100×10×16 mm with different L_e

(a) L_e = 1.0 m with λ = 25.30

Specimen labelling	P_{FEA} (kN)	Normalized #	Failure mode
280×100×10×16-1.0-ϕ0	2235.6	1.000	Plastic yielding
280×100×10×16-1.0-ϕ3	2245.1	1.004	Plastic yielding
280×100×10×16-1.0-ϕ10	2236.0	1.000	Plastic yielding
280×100×10×16-1.0-ϕ15	2243.3	1.003	Plastic yielding
280×100×10×16-1.0-ϕ20	2241.7	1.003	Plastic yielding
280×100×10×16-1.0-ϕ30	2236.2	1.000	Plastic yielding
280×100×10×16-1.0-ϕ40	2233.1	0.999	Plastic yielding
280×100×10×16-1.0-ϕ50	2221.2	0.994	Plastic yielding
280×100×10×16-1.0-ϕ60	2211.1	0.989	Plastic yielding
280×100×10×16-1.0-ϕ70	2199.2	0.984	Plastic yielding
280×100×10×16-1.0-ϕ80	2179.8	0.975	Plastic yielding
280×100×10×16-1.0-ϕ90	2165.3	0.969	Plastic yielding
280×100×10×16-1.0-ϕ100	2149.6	0.962	Plastic yielding
280×100×10×16-1.0-ϕ110	2133.3	0.954	Plastic yielding
280×100×10×16-1.0-ϕ120	2115.3	0.946	Plastic yielding

Note: "#" means the ultimate loads of columns normalized by the ultimate loads of the column without pre-twisting.

(b) L_e = 1.5 m with λ = 37.94

Specimen labelling	P_{FEA} (kN)	Normalized	Failure mode
280×100×10×16-1.5-ϕ0	2163.5	1.000	Plastic yielding
280×100×10×16-1.5-ϕ3	2163.6	1.000	Plastic yielding
280×100×10×16-1.5-ϕ10	2164.7	1.001	Plastic yielding
280×100×10×16-1.5-ϕ15	2166.1	1.001	Plastic yielding
280×100×10×16-1.5-ϕ20	2167.6	1.002	Plastic yielding
280×100×10×16-1.5-ϕ30	2170.7	1.003	Plastic yielding
280×100×10×16-1.5-ϕ40	2166.0	1.001	Plastic yielding
280×100×10×16-1.5-ϕ50	2158.1	0.998	Plastic yielding
280×100×10×16-1.5-ϕ60	2147.9	0.993	Plastic yielding
280×100×10×16-1.5-ϕ70	2133.1	0.986	Plastic yielding
280×100×10×16-1.5-ϕ80	2118.8	0.979	Plastic yielding
280×100×10×16-1.5-ϕ90	2105.6	0.973	Plastic yielding
280×100×10×16-1.5-ϕ100	2085.1	0.964	Plastic yielding
280×100×10×16-1.5-ϕ110	2065.9	0.955	Plastic yielding
280×100×10×16-1.5-ϕ120	2055.4	0.950	Plastic yielding

(c) L_e = 2.0 m with λ = 50.59

Specimen labelling	P_{FEA} (kN)	Normalized	Failure mode
280×100×10×16-2.0-ϕ0	1925.6	1.000	Flexure buckling
280×100×10×16-2.0-ϕ3	1925.8	1.000	Flexure buckling
280×100×10×16-2.0-ϕ10	1927.5	1.001	Flexure buckling
280×100×10×16-2.0-ϕ15	1929.5	1.002	Flexure buckling
280×100×10×16-2.0-ϕ20	1931.8	1.003	Flexure buckling
280×100×10×16-2.0-ϕ30	1936.3	1.006	Flexure buckling
280×100×10×16-2.0-ϕ40	1940.1	1.008	Flexure buckling
280×100×10×16-2.0-ϕ50	1943.1	1.009	Flexure buckling
280×100×10×16-2.0-ϕ60	1945.1	1.010	Flexure buckling
280×100×10×16-2.0-ϕ70	1945.4	1.010	Flexure buckling
280×100×10×16-2.0-ϕ80	1944.0	1.010	Flexure buckling
280×100×10×16-2.0-ϕ90	1939.0	1.007	Flexure buckling
280×100×10×16-2.0-ϕ100	1929.6	1.002	Flexure buckling
280×100×10×16-2.0-ϕ110	1914.4	0.994	Flexure buckling
280×100×10×16-2.0-ϕ120	1893.4	0.983	Flexure buckling

(d) L_e = 3.0 m with λ = 75.89

Specimen labelling	P_{FEA} (kN)	Normalized	Failure mode
280×100×10×16-3.0-ϕ0	1453.7	1.000	Flexure buckling
280×100×10×16-3.0-ϕ3	1455.2	1.001	Flexure buckling
280×100×10×16-3.0-ϕ10	1464.3	1.007	Flexure buckling
280×100×10×16-3.0-ϕ15	1474.3	1.014	Flexure buckling
280×100×10×16-3.0-ϕ20	1484.4	1.021	Flexure buckling
280×100×10×16-3.0-ϕ30	1504.5	1.035	Flexure buckling
280×100×10×16-3.0-ϕ40	1524.7	1.049	Flexure buckling
280×100×10×16-3.0-ϕ50	1546.2	1.064	Flexure buckling
280×100×10×16-3.0-ϕ60	1569.8	1.080	Flexure buckling
280×100×10×16-3.0-ϕ70	1596.2	1.098	Flexure buckling
280×100×10×16-3.0-ϕ80	1626.4	1.119	Flexure buckling
280×100×10×16-3.0-ϕ90	1658.6	1.141	Flexure buckling
280×100×10×16-3.0-ϕ100	1683.6	1.158	Flexure buckling
280×100×10×16-3.0-ϕ110	1686.0	1.160	Flexure buckling
280×100×10×16-3.0-ϕ120	1672.2	1.150	Flexure buckling

(e) L_e = 4.0 m with λ = 101.18

Specimen labelling	P_{FEA} (kN)	Normalized	Failure mode
280×100×10×16-4.0-ϕ0	1163.3	1.000	Flexure buckling
280×100×10×16-4.0-ϕ3	1166.7	1.003	Flexure buckling
280×100×10×16-4.0-ϕ10	1190.9	1.024	Flexure buckling
280×100×10×16-4.0-ϕ15	1210.1	1.040	Flexure buckling
280×100×10×16-4.0-ϕ20	1226.7	1.055	Flexure buckling
280×100×10×16-4.0-ϕ30	1253.1	1.077	Flexure buckling
280×100×10×16-4.0-ϕ40	1273.4	1.095	Flexure buckling
280×100×10×16-4.0-ϕ50	1287.8	1.107	Flexure buckling
280×100×10×16-4.0-ϕ60	1313.7	1.129	Flexure buckling
280×100×10×16-4.0-ϕ70	1361.8	1.171	Flexure buckling
280×100×10×16-4.0-ϕ80	1406.4	1.209	Flexure buckling
280×100×10×16-4.0-ϕ90	1422.0	1.222	Flexure buckling
280×100×10×16-4.0-ϕ100	1414.7	1.216	Flexure buckling
280×100×10×16-4.0-ϕ110	1396.6	1.201	Flexure buckling
280×100×10×16-4.0-ϕ120	1370.5	1.178	Flexure buckling

Table 7: Effects of ϕ on column behaviour for specimens with different ratios of h/b and L_e

(a) Section 100×100×10×16 mm with h/b = 1.0

Specimen labelling	λ	P_{FEA} (kN)	Normalized	Failure mode
100×100×10×16-1.0-ϕ0	28.97	1194.1	1.000	Plastic yielding
100×100×10×16-1.0-ϕ20		1194.0	1.000	Plastic yielding
100×100×10×16-1.0-ϕ40		1193.5	0.999	Plastic yielding
100×100×10×16-1.0-ϕ60		1192.8	0.999	Plastic yielding
100×100×10×16-1.0-ϕ80		1191.8	0.998	Plastic yielding
100×100×10×16-1.0-ϕ90		1191.2	0.998	Plastic yielding
100×100×10×16-1.0-ϕ100		1190.4	0.997	Plastic yielding
100×100×10×16-4.0-ϕ0	115.89	516.2	1.000	Flexure buckling
100×100×10×16-4.0-ϕ20		517.2	1.002	Flexure buckling
100×100×10×16-4.0-ϕ40		519.2	1.006	Flexure buckling
100×100×10×16-4.0-ϕ60		522.6	1.012	Flexure buckling
100×100×10×16-4.0-ϕ80		525.4	1.018	Flexure buckling
100×100×10×16-4.0-ϕ90		526.3	1.020	Flexure buckling
100×100×10×16-4.0-ϕ100		526.6	1.020	Flexure buckling

(b) Section 150×100×10×16 mm with h/b = 1.5

Specimen labelling	λ	P_{FEA} (kN)	Normalized	Failure mode
150×100×10×16-1.0-ϕ0	27.29	1468.5	1.000	Plastic yielding
150×100×10×16-1.0-ϕ20		1468.1	1.000	Plastic yielding
150×100×10×16-1.0-ϕ40		1466.8	0.999	Plastic yielding
150×100×10×16-1.0-ϕ60		1464.3	0.997	Plastic yielding
150×100×10×16-1.0-ϕ80		1462.0	0.996	Plastic yielding
150×100×10×16-1.0-ϕ90		1460.5	0.995	Plastic yielding
150×100×10×16-1.0-ϕ100		1456.1	0.992	Plastic yielding
150×100×10×16-4.0-ϕ0	109.16	704.4	1.000	Flexure buckling
150×100×10×16-4.0-ϕ20		724.8	1.029	Flexure buckling
150×100×10×16-4.0-ϕ40		762.2	1.082	Flexure buckling
150×100×10×16-4.0-ϕ60		800.9	1.137	Flexure buckling
150×100×10×16-4.0-ϕ80		831.4	1.180	Flexure buckling
150×100×10×16-4.0-ϕ90		839.9	1.192	Flexure buckling
150×100×10×16-4.0-ϕ100		843.4	1.197	Flexure buckling

(c) Section 200×100×10×16 mm with h/b = 2.0

Specimen labelling	λ	P_{FEA} (kN)	Normalized	Failure mode
200×100×10×16-1.0-ϕ0	26.28	1746.0	1.000	Plastic yielding
200×100×10×16-1.0-ϕ20		1745.2	1.000	Plastic yielding
200×100×10×16-1.0-ϕ40		1736.9	0.995	Plastic yielding
200×100×10×16-1.0-ϕ60		1733.0	0.993	Plastic yielding
200×100×10×16-1.0-ϕ80		1726.8	0.989	Plastic yielding
200×100×10×16-1.0-ϕ90		1722.7	0.987	Plastic yielding
200×100×10×16-1.0-ϕ100		1717.6	0.984	Plastic yielding
200×100×10×16-4.0-ϕ0	105.19	889.0	1.000	Flexure buckling
200×100×10×16-4.0-ϕ20		931.8	1.048	Flexure buckling
200×100×10×16-4.0-ϕ40		986.3	1.109	Flexure buckling
200×100×10×16-4.0-ϕ60		1024.1	1.152	Flexure buckling
200×100×10×16-4.0-ϕ80		1040.0	1.170	Flexure buckling
200×100×10×16-4.0-ϕ90		1041.1	1.171	Flexure buckling
200×100×10×16-4.0-ϕ100		1038.3	1.168	Flexure buckling

(d) Section 280×100×10×16 mm with h/b = 2.8

Specimen labelling	λ	P_{FEA} (kN)	Normalized	Failure mode
280×100×10×16-1.0-ϕ0$^{\wedge}$	25.30	2235.6	1.000	Plastic yielding
280×100×10×16-1.0-ϕ20$^{\wedge}$		2241.7	1.003	Plastic yielding
280×100×10×16-1.0-ϕ40$^{\wedge}$		2233.1	0.999	Plastic yielding
280×100×10×16-1.0-ϕ60$^{\wedge}$		2211.1	0.989	Plastic yielding
280×100×10×16-1.0-ϕ80$^{\wedge}$		2179.8	0.975	Plastic yielding
280×100×10×16-1.0-ϕ90$^{\wedge}$		2165.3	0.969	Plastic yielding
280×100×10×16-1.0-ϕ100$^{\wedge}$		2149.6	0.962	Plastic yielding
280×100×10×16-4.0-ϕ0$^{\#}$	101.18	1163.3	1.000	Flexure buckling
280×100×10×16-4.0-ϕ20$^{\#}$		1226.7	1.055	Flexure buckling
280×100×10×16-4.0-ϕ40$^{\#}$		1273.4	1.095	Flexure buckling
280×100×10×16-4.0-ϕ60$^{\#}$		1313.7	1.129	Flexure buckling
280×100×10×16-4.0-ϕ80$^{\#}$		1406.4	1.209	Flexure buckling
280×100×10×16-4.0-ϕ90$^{\#}$		1422.0	1.222	Flexure buckling
280×100×10×16-4.0-ϕ100$^{\#}$		1414.7	1.216	Flexure buckling

Note: "$^{\wedge}$": presented in Table 6 (a); "$^{\#}$": presented in Table 6 (e).

(e) Section 120×100×10×16 mm with h/b = 1.2

Specimen labelling	λ	P_{FEA} (kN)	Normalized	Failure mode
120×100×10×16-4.0-ϕ0	112.73	591.5	1.000	Flexure buckling
120×100×10×16-4.0-ϕ20		599.9	1.014	Flexure buckling
120×100×10×16-4.0-ϕ40		617.3	1.044	Flexure buckling
120×100×10×16-4.0-ϕ60		636.3	1.076	Flexure buckling
120×100×10×16-4.0-ϕ80		651.5	1.101	Flexure buckling
120×100×10×16-4.0-ϕ90		656.2	1.109	Flexure buckling
120×100×10×16-4.0-ϕ100		658.8	1.114	Flexure buckling

Table 8: Effects of ϕ on column behaviour for specimens with pin-end boundary conditions and free rotation about both major and minor axes

Specimen labelling	λ	P_{FEA} (kN)	Normalized	Failure mode
280×100×10×16-4.0-ϕ0	101.18	1163.3	1.000	Flexure buckling
280×100×10×16-4.0-ϕ3		1164.5	1.001	Flexure buckling
280×100×10×16-4.0-ϕ15		1185.5	1.019	Flexure buckling
280×100×10×16-4.0-ϕ20		1197.8	1.030	Flexure buckling
280×100×10×16-4.0-ϕ40		1252.4	1.077	Flexure buckling
280×100×10×16-4.0-ϕ60		1293.2	1.112	Flexure buckling
280×100×10×16-4.0-ϕ80		1405.2	1.208	Flexure buckling
280×100×10×16-4.0-ϕ100		1409.5	1.212	Flexure buckling
280×100×10×16-4.0-ϕ120		1362.0	1.171	Flexure buckling